THE HEBREW UNIVERSITY
OF JERUSALEM

ES-26-01

THE MINISTRY OF NATIONAL
INFRASTRUCTURES
GEOLOGICAL SURVEY OF ISRAEL

GSI/33/01

Dating Tectonic Events Using Damaged Cave Deposits: Soreq and Har-Tuv Caves, Israel

Elisa Kagan [1,2]
Amotz Agnon [1]
Miryam Bar-Matthews [2]
Avner Ayalon [2]

[1] Hebrew University of Jerusalem
[2] Geological Survey of Israel

Annual report submitted to the the ministry of national infrastructures

Jerusalem, November 2001

THE HEBREW UNIVERSITY
OF JERUSALEM

ES-26-01

THE MINISTRY OF NATIONAL
INFRASTRUCTURES
GEOLOGICAL SURVEY OF ISRAEL

GSI/33/01

Dating Tectonic Events Using Damaged Cave Deposits: Soreq and Har-Tuv Caves, Israel

Elisa Kagan [1,2]
Amotz Agnon [1]
Miryam Bar-Matthews [2]
Avner Ayalon [2]

[1] Hebrew University of Jerusalem
[2] Geological Survey of Israel

Annual report submitted to the the ministry of national infrastructures

Jerusalem, November 2001

Acknowledgements

We would like to thank Aaron Kaufman for his knowledge, patience, and time with regard to alpha dating. We thank Irena Segal for her technical assistance and her immediate willingness to solve any problem with regard to the alpha sample preparation and ICP measurements. We thank Bettina Schilman for the stable isotope mass spectrometric measurements. We thank Dan Asael and Anton Vaks for their dedicated work in the alpha sample preparation and dating laboratories. We thank Bassam Gahleb, from the University of Quebec at Montreal, for the TIMS dating. None of this could have been done without the dedicated field and laboratory assistance of the technicians of the Survey, above all Eli Ram, Shlomo Ashkenazi, and Robert. We thank Bat- Sheva Cohen for her time and eagerness to help. We are grateful to Hani Alon and Ami Peled at the Soreq Cave Nature Reserve for their assistance and consideration with our work.

1. Introduction

Quaternary studies are valuable for the comprehension of present-day geological processes, including tectonic processes that produce earthquakes (Yeats et al., 1997; McCalpin, 1996). However, recent Quaternary deposits are not always available in all places where large earthquakes have struck. The search for new markers that could have recorded co-seismic events has led to the use of cave deposits, known as speleothems, as a valuable tool. These markers allow detection and study of paleoseismic events, large and small, in areas where return rates are long and historic evidence is not sufficient. The use of karst in active tectonic research is indispensable in regions with no other Quaternary deposits, while in Israel there are various other earthquake markers that can be compared to (e.g. Amit et al., 1996, 1999; Enzel et al., 1996, 2000; Marco et al., 1996; Ellenblum et al., 1998; Ken-Tor et al., 2001).

The Soreq Cave near Jerusalem, along with other caves and karstic features in Israel, offers an excellent opportunity to investigate this field of study. The Soreq Cave has been studied intensively and shows continuous growth of speleothems for the last 185, 000 (Bar-Matthews et al., 2000b) and probably the past 350,000 years (Bar-Matthews and Ayalon, unpublished data). It contains a vast amount of fallen cave deposits of all types and sizes, which can provide information on the seismic history of the region, including dates of events, local intensity, and other physical data pertaining to underground earthquake damage. The U-series dating of fallen speleothems and of deposits that have grown on them will accurately place the causative events into the regional seismic chronological record. The primary goal of this work is to document and date the seismic events recorded in karstic features during the Late Quaternary. This study attempts to complement the relatively long historical earthquake catalogue (Amiran et al., 1994; Guidoboni, 1994) and the late Pleistocene and early Holocene events recorded by sediments in the Dead Sea area (Marco et al., 1996; Ken-tor et al., 2001). Because of the time range of the U-series dating method (350-500 kyr) (Edwards et al., 1987; Chen et al., 1990) and the extensive karstic record available, this study includes previously undated earlier tectonic events.

Tectonic and Paleoseismic Use of Speleothems

Caves create an environment protected from most erosive activity. The calcite and detrital deposits have laminar growth patterns and therefore make the endokarst an advantageous medium for the recording and preservation of delicate evidence of earthquakes. Speleothems can be dated with various methods, mainly radioactive techniques, and it is therefore possible to establish a chronology of tectonic events.

Earthquakes can affect speleothems in different ways: collapse inside caves due to ground motions, change in stalagmite or stalactite growth axis in response to tilt, and creation or opening and closing of cracks according to their orientation relative to the seismotectonic stress field (Forti and Postpischl, 1984; Forti, 1998; Gilli, 1999a; Gilli et al., 1999). These effects can aid in the evaluation of major paleoseismic events with respect to (1) relative and absolute dating and return rates, (2) location and epicenter, and (3) intensity. Jibson (1996) recommends applying stability analysis to speleothems, whose dynamic stability can easily be modeled, to estimate the ground shaking required to cause failure.

A variety of methods concentrate on different effects that ancient earthquakes and other tectonic movements have had on caves and their deposits. Forti and Postpischl (1984) show that a speleothem can be treated as a natural pendulum. The growth axis of the stalagmite records the vertical direction at time of deposition, which, if stable in time, would result in a linear segment. They attribute observed deviations to local perturbations or swinging movements of the plate to which the system is fixed.

Postpischl et al. (1991) used the relative chronology of discontinuities in the growth axes of two stalagmites from Italy to correlate fifteen anomalies with historical earthquakes from the detailed Bologna catalogue. In the same study, at a different cave, they attempted radiometric dating using ^{14}C and U/Th methods. They concluded that the chemical efficiency was "poor", as is the reliability of the results, since the geochemical system recorded in the internal structure of some of the speleothems was reset during periods of flooding. Their study lacked reliable radiometric ages.

Morinaga et al. (1994) demonstrated the possibility of inferring paleoseismicity from paleomagnetic dating of speleothems from western Japan. Samples were taken from fallen blocks of limestone bedrock. The authors explain that in areas of active seismicity,

earthquakes can contribute to a "ready-to-collapse" condition and may trigger block falls. Using the weak but stable remanent magnetization of speleothems they determined the paleosecular variation (PSV) of the geomagnetic field and by comparison with the standard curve, the time of growth could be established. Three ages of events were obtained: 6000, 2500, and 2000 years B.P. Practical application of this method in Japan is restricted to the last tens of thousands of years, for which the standard PSV of the geomagnetic field direction is known. Moreover, this method is applicable only in the case that the samples are known to be in the age range of the standard curve, since older specimens may have PSV values equal to those of the standard curve and therefore will give incorrect apparently young ages.

Lemeille et al. (1999) studied the deformations recorded by speleothems in the epicentral zone of the 1356 A.D. earthquake in Basel, Switzerland. This was one of the most destructive historical earthquakes known in Western Europe. Despite the large amount of damage (intensity VII-IX) there is no known surface rupture, nor superficial displacement. Yet, in the study cave breakages, growth anomalies, and displacements were observed. Four samples were dated in order to determine simultaneity of the collapse events. One of these ages corresponds to the 1356 A.D. earthquake. Results showed that the activities of U and Th in their samples were too low to give precise $^{230}Th/^{234}U$ ages (alpha counting), but perhaps are suitable for thermal ionization mass spectrometry (T.I.M.S.) U/Th dating, which was not done. Radiocarbon dating provided four ages of bases of regrowths taken from fallen blocks and from stumps of severed stalagmites. One of these ages corresponds to the 1356 A.D. earthquake.

Effects of recent, instrumentally recorded earthquakes may be investigated, with the advantage of knowing the exact age of the damage and magnitude of the event. Gilli et al. (1999) studied eight caves of Saint-Paul-de-Fenouillet (eastern Pyrenees, France) after the 5.2 magnitude earthquake that occurred on February 18, 1996. Great variability was noticed in the damage to the different caves; solely one cave displayed an abundance of broken soda-straws (macaroni-type stalactites) and massive speleothem destruction. This cave is the topographically highest one (850 m) and is located on a limestone crest. In contrast, caves closer to the epicenter but at elevations below 400 m. showed no damage. Consequently, the authors supposed a site effect amplification of ground motion. In the affected cave they analyzed the directions of the fragments on the floor and found a

dominant orientation (E-W). An attempt was made to model soda-straw behavior in order to evaluate the necessary conditions for breakage during an earthquake.

Flowstone is an excellent candidate for study, since in many cases it behaves as a floor and fossilizes objects that have fallen. In a Monaco cave, Gilli (1999a) drilled cores in a flowstone and noted three to five levels of collapsed sodastraws in a section of the polished sample. The author attributed two of the levels to catalogued historical earthquakes (1887 AD and 1564 AD).

In order to use speleothems as recorders of tectonic events it must be established that their disturbed state, whether it be displaced, non-linear, broken, or otherwise damaged, is a result of tectonic occurrences, and not of static load, anthropogenic, climatic, hydrologic, nor any other non-tectonic occurrence. Possible nonseismic damage of speleothems has been investigated by Gilli (1999b) in the Ribiere cave, France. He lists examples of causes for non-coseismic breakings: ice fillings, human causes, underground bears, clay subsidence, and sediment creep.

The following non-coseismic causes of damage to caves can be refuted in the case of the Soreq Cave and most caves in Israel:

1. Ice movements: as opposed to many higher latitude caves in Europe, there has never been ice cover during the time period being investigated and therefore ice movements are out of the question as causes of collapse.

2. Anthropogenic sources: recent damage by quarrying at the Hartuv quarry or development of the cave can be distinguished from less recent seismic events by morphological assessment (Crispim, 1999) and dating; observations indicate that as a result of the quarrying explosions only macaroni-type speleothems have fallen, and perhaps minor cracking of deposits had occurred (except at the entrance) (Bar-Matthews, unpublished data).

3. Bears: in historic times bears lived in Israel, however in the study caves there is no evidence of mammal presence; the study caves were closed to the exterior and only recently exposed by quarrying.

4. Subsidence: no evidence of subsidence is known from the vicinity of the caves.

5. Sediment creep: there is only one minor area of the Soreq Cave that has sediment fill, however it is restricted to a high point and shows no signs of creep.

As these points are eliminated, we may assume, as a working hypothesis, that earthquakes caused the observed damage. This hypothesis is tested below by correlation with other paleoseismic works.

This study can complement other ongoing paleoseismic studies in the region, which until now mainly confronted the issues of earthquakes that caused surface rupture in the Dead Sea Rift region (e.g., Marco & Agnon, 1995; Marco et al., 1996; Amit et al., 1996; Enzel et al., 1996, 2000; Ellenblum et al., 1998; Ken-Tor et al., 2001). Recent studies have brought to light the "clustering" behavior of earthquakes on time scales of ten thousand years (Marco et al., 1996), and because of which short records cannot be counted on for the evaluation of seismic hazards. This research will add information to the long-term geological record.

The Soreq Cave, 15 kilometers west of Jerusalem, has been the subject of petrographic, paleoclimatic, and karstic study since its discovery in 1968 (e.g., Asaf, 1975; Even, 1983; Bar Matthews et al., 1993, 1997, 1999, 2000a,b; Frumkin et al., 1994; Kaufman et al., 1998; Ayalon et al., 1999). However, no systematic paleoseismic investigations or dating of tectonic events have been carried out. The Soreq Cave and the Har-Tuv Cave are located about 60 km west of the Dead Sea Fault and can provide information on the extent of damage from earthquakes associated with ruptures on the transform. Smaller intraplate earthquakes may be represented as well.

2. Geological Background

Location, Stratigraphy and Structure

This study has been carried out at the Soreq and Har-Tuv Caves, both of which are in the vicinity of the Avshalom Nature Reserve, 15 km west of Jerusalem (Fig.1). The Soreq Cave is strewn with an enormous amount of fallen cave deposits and has been the subject of paleoclimatic and karst study since its discovery. For these reasons we have chosen it for our paleotectonic work. In 1968, the cave was first exposed as a result of quarrying at the Hartuv Quarry. It is situated on the western flank of the Nes Harim pass at coordinate 152220/129260 (Asaf, 1975; Eisenstein, 1970), 395 m above sea level, and five kilometers northeast of the town of Beit Shemesh. The Har-Tuv Cave is less than one kilometer from Soreq and has nearly identical geological and climatic conditions. It was also recently

uncovered by quarrying activities. The reason we chose to work with two nearby caves was for the prospect correlation. One way to confirm that a collapse event in the Soreq Cave was the result of an earthquake is by discovering that the same event caused a collapse in an additional cave. The Har-Tuv Cave is a shallower cave, which possibly makes it more sensitive to seismic waves, and may be vulnerable to smaller tectonic events. Furthermore, the Har-Tuv Cave is in an active part of the Har-Tuv Quarry, is not in the nature reserve, and is intended for destruction. This fact encourages sampling in this cave, in preference to the Soreq Cave.

Fink (1962), Arkin et al. (1965), and Lasman (1965) mapped the area surrounding the Soreq and Har-Tuv Caves. This area is a part of the western fold of the Judean Anticline, whose axial plane strikes NNE. A steep western flank dipping 15^0-30^0 and a shallow eastern flank characterize the anticline. Variations in the dip and strike are due to local folding and faulting within the major anticline. The exposed rocks are of the Upper Cenomanian Judea Group, comprising mainly limestones, dolomites and marls. The formations outcropping near the cave include Aminadav, Weradim, and Bina. The following review of the fractures, faults, lithology, and karstic features of the study area is given by Arkin (1980). The main orientations of fractures are 150^0, 110^0 and 75^0, while secondary fractures are oriented 180^0 and 35^0. In the study area two fault systems are prominent. One system belongs to the Judean anticline and comprises faults that are a number of kilometers long, have a few meters displacement, and strike NE-SW, NW-SE, and NS. The faults of this system are a result of extension. A second system is associated with breccias, fracturing, and normal faults striking NNW-SSE and E-W. This system is also associated with the anticline and usually forms a belt a few kilometers long, and tens of meters wide. The Soreq Cave has formed entirely in the Upper Cenomanian Weradim Formation. Along with Bina and Aminadav formations, the Weradim Fm. makes up the main aquifer of the mountain region. In the study area, the formation varies from well bedded to massive gray dolomite, averaging a thickness of 60 m. The beds range from 0.4 to 3 m thickness, are normally well pronounced, and the amount of their dip is 20^0-25^0 towards the west. The density of the rock ranges from 2.51 to 2.73 g/cm^3. There is a mostly cemented breccia at the bottom part of the formation reaching a thickness of 10 m in places. Most of the aggregate quarries in the region are developed in the Weradim Fm.

Karst

Soreq Cave: Asaf (1975) reviews the dimensions and features of the Soreq Cave. The cave is elongated in the NW- SE direction with an average length of 80 m and an average width of 60 m (Fig. 2, Fig. 3).The area is approximately 5000 m^2, with a volume of 25,440 – 26,000 m^3. The thickness of the roof, from cave ceiling to surface, ranges from 12 m to 50 m, with an average volume of 150,000 m^3 and weight of 400,000 tons. The cave floor slopes irregularly downwards to the south at an average angle of 22^0. The floor is made up of flowstone, stalagmites, fallen speleothems, and locally some soil. The ceiling is composed of dolomite bedrock, cemented breccia, and speleothems. Asaf (1975) comments on the large amount of fractures on the ceiling of the cave; he notes that some of them are filled with red sediments and comments on the probability that these fractures connect the cave to the ground surface. He describes curtain-type stalactites that grow below the fractures on the ceiling and form walls. These walls divide the cave into "rooms" or "halls".

The Soreq Cave may have formed during the Miocene to Pleistocene, as a consequence of hydrological activity during regression of the Miocene sea. This lowering of the erosion base exposed rocks of the Judea Group by the incision of deep canyons. Karst was likely to have formed mainly near the main drainage systems of the Judean and Hebron mountains, such as the ancient Soreq River (Arkin, 1980). Frumkin et al. (1994) state that the Soreq Cave probably has a phreatic origin (formed below the water table). Today it is fossil, situated above the present water table. After a drop in the water table the cave began a period of erosion, deposition of speleothems, and collapse. Deposition of speleothems has probably been continuous for at least the past 300 ky (Bar-Matthews and Ayalon, unpublished data) and certainly for the past 185 ky (Bar-Mathews et al., 2000b).

The sediments in the cave have two origins: allochtonous and autochthonous. The allochtonous material includes mud, some pebbles, and a small number of land snails. This is especially noticeable in the north area where there is a 4 m high pile of mud below a large fracture. The autochtonic forms can be divided into primary material that has not undergone dissolution and recrystalisation, such as the collapsed blocks of dolomite, and secondary formations (speleothems) that have formed by precipitation inside the cave, from the calcite-saturated percolating water dripping into the cave. These speleothems have a wide range of forms that include stalactites, stalagmites, curtains, flowstones, rimstones,

helectites, globulite corals, and calcite films. They are composed mainly of low-magnesium calcite.

Har-Tuv Cave: A basic map of the Har-Tuv Cave was drawn by Disni (1997) and enhanced in this work (Fig. 4). It is part of the same system of karstic caves described above. At the entrance to the cave there is a fault that dips 75/035, showing slickensides orienting 125^0. The cave itself is fairly horizontal. The thickness of bedrock and soil above the cave is approximately 30 m. It is a small cave, about 20 m long and at most 7 m wide. There are two non-natural entrances, formed by quarry explosions. Fractures observable on the cave ceiling orient mainly 110^0. Bedding plane are visible on the cave ceiling. There are many standing speleothem columns and some broken ones. There is an abundance of ceiling collapses, mostly covered with stalagmite growth. There is also an area covered in a thick layer of flowstone. Inside a fresh water pool, surrounded by immersed stalactites, lie a number of fallen cave deposits and ceiling pieces.

Seismotectonics of the Region

Salamon et al. (1996) analyzed the relationship between seismicity and tectonics the Sinai subplate, bordered by the Suez Rift in the southwest, the Dead Sea Transform in the east, and the Cypriotic Arc zone in the north. The major seismogenic element of the area is the Levant fracture zone, which in our area includes the following seismogenic areas: the Dead Sea Rift, the Carmel Fault, the Gulf of Eilat (Aqaba), the offshore of Israel, the Gulf of Suez, and the Cypriotic Arc. It is a heterogeneous tectonic region, with compressional, extensional, and transformal deformation zones. In northern Israel the seismogenic belt is rather wide, while south of the Carmel Fault the belt narrows and epicenters are concentrated in the deep depressions of the Dead Sea and Gulf of Eilat areas. Focal mechanisms of large events in the Dead Sea Transform mainly show strike slip or normal movement, and most are shallow.

Although not directly on any of the seismic features, the Jerusalem area has been affected by many earthquakes. Being continuously populated and a major religious and political center throughout historical times, the record of these earthquakes is extensive and well catalogued (Ben Menahem, 1991; Ambraseys et al., 1994; Amiran et al., 1994), with epicenters being estimated as Dead Sea Rift area, Carmel Fault, and even as far as the

Cypriotic Arc. At present it is not possible to exclude sources from interplate events originating in closer faults.

Return rates are estimated by a number of authors for the Dead Sea transform:

1) Ben Menahem (1991): 1500 yrs, southern half of DST: M max=7.3

2) Marco et al. (1996): ~1600 yrs for $M_L \geq 5.5$

3) Reches and Hoexter (1981): Jericho Fault: 779 yrs (between two historical events)

4) Rotstein (1987): 280 yrs, N. Jordan Valley; 262 yrs, S. Jordan Valley

5) Salamon et al. (1996): 385 yrs, DST: M=7:, 1250 yrs, M=7.5:, 3330 yrs, M=8

Yet, the Soreq and Har-Tuv area, like Jerusalem, is affected by a number of source-faults, as documented in historical catalogues (Ben Menahem, 1991; Ambraseys et al., 1994; Amiran et al., 1994). Avni (1999) presents an isoseismal map of the 1927 earthquake near Jericho using the MSK (Medvedev Sponheur Karnik) intensity scale (Fig. 5). The Jerusalem- Beit Shemesh area falls within the I=VII isoseismal zone. This intensity is associated with the following effects: difficulty in standing; slight damage to good construction; moderate damage to medium construction; heavy damage to poor construction; cracks in roads and stone walls; landslips of roadway on steep slopes; change in well water levels; some damage to pipelines (Bath, 1973).

Modern seismic monitoring has been comprehensive since 1981, when the seismograph network was implemented in Israel. This century, in the Jerusalem- Beit Shemesh area, shocks of up to magnitude M_L=3.5 are recorded.

3. Research Objectives

The primary objectives of this study are the following:

1. Dating of collapses of ceiling blocks and speleothems by radiometry of the calcite covering them.
2. Comparison of collapse ages with those of historically recorded earthquakes and with those of sedimentologically recorded earthquakes in the past 70, 000 years.
3. Testing the viability of karstic features as paleoseismic indicators.

In addition to these main goals, this work may have implications regarding hiatuses of speleothem growth as indicators of tectonic opening and closing of fractures, and

correlation of these hiatus periods with periods of earthquake activity in the Dead Sea Rift region; contribution to the understanding of earthquake-induced damage to underground features; contribution to the knowledge of the seismic history of a region somewhat removed from the immediate fault zone.

4. Methods

Field Work

The survey map drawn by Shrir and Shrir (1969) for the Nature Reserves Authority served as the basis for the many features that have been mapped in this work. The orientation and length of the fractures in and around the cave were mapped (Fig. 3). Collapsed and deformed speleothems and ceiling blocks have been measured and described in detail. The orientation of each fall has been recorded, as well as where it may have fallen from, if it is cemented into position by calcite growth, and if there are speleothem regrowths on it that can be dated. Other features such as faults and cracks have been documented.

Speleothem Sampling

Sampling in the caves was done by a hand-held pneumatic drill, with a diameter of 5-10 cm, and with a hammer and chisel. Forty-five drilled cores and hand specimens were collected in the Soreq Cave and 25 were collected in the Har-Tuv Cave. Samples include fallen speleothems and bedrock ceilings, stalagmites that have grown on them before and after collapse, and cores of flowstone floor. We have made the outmost effort to minimalize damage to the caves by taking samples out of sight of the walking path, and by filling in holes with a lime mixture. Preliminary identification of the collapse contact within samples was done in the field. Schematic diagrams were drawn of demonstrative collapses.

Alpha dating

Preparation of Samples for Dating

The preparation and dating of samples were performed at the laboratories of the Geochemistry Department of the Geological Survey of Israel. The speleothems were first

sawed in half using a 2mm diamond saw parallel to growth axis in order to clearly expose lamina. One half is used for dating, while the other half is kept for isotopic profile sampling and for possible future use. Lamina and collapse contacts are recognized and labeled. The sample was examined for recrystalisation and if any was found the sample was not further used. Lamina required for dating were identified and separated from the speleothem using a 1 mm diamond saw. At this stage it was imperative to keep separate the pre-collapse and post-collapse lamina, and especially the bedrock pieces, in order to prevent contamination of differently aged pieces. Petrographic examinations and XRD analyses were performed only in cases of suspicion of bedrock embedded in the crystal. Detrital matter was removed by crushing with mortar and pestle, agitating in distilled water with a high-powered Sonicator ultrasonic processor (Minosonix) for about three minutes, and then immediately decanting the supernate (water and suspended particles). This procedure was repeated 3 to 4 times and the sample was then dried. A Perkin-Elmer/Sciex Elam 6000 ICP-MS (Inductively Coupled Plasma Mass Spectrometer) was then used to measure thorium and uranium concentrations (Halicz et al., 1997) in order to know how much sample is needed for dating and as a verification of alpha results. In preparation for measuring by ICP, 100 mg of powdered sample was dissolved in 2 cc of 1:5 HNO_3 and then 8 cc of 0.1 N HNO_3 were added. After total dissolution 0.1 cc of Rhenium is added as an internal standard. If ICP measurement and alpha counting did not produce the same U and Th concentration results, the samples were dated a second time.

Since ^{230}Th and ^{234}U emit alpha particles of very similar energy it is necessary to separate uranium and thorium isotopes chemically prior to alpha counting. Th and U are chemically separated from the host matrix (speleothem calcite) and from one another by the following procedure (Kaufman and Broecker, 1965; Gascoyne et al., 1978; Lally, 1992).

1. Crushed sample dissolution in 8N HNO_3
2. Introduction of ^{232}U-^{228}Th spike (500 ppb)
3. Addition of Fe^{3+} carrier (7g/100cc $FeCl_3$)
4. Hydroxide precipitation of U and Th with $Fe(OH)_3$ and dissolution in HCl
5. U and Th separation by HCl conditioned anion-exchange chromatography (Dowex AG 1X8 resin column)
6. Th and Al separation by HNO_3 conditioned anion-exchange chromatography (Dowex AG 1X8 resin column)

7. Isopropyl ether extraction for separation of U and Fe

8. U and Th isolation by solvent extraction with thenoyl-trifluoro-acetone (TTA)

The final separated fractions are evaporated on heated (~150^0) stainless steel discs in order to obtain a very thin and even layer. The discs are then heated to 800^0 in order to oxidize any remaining organic matter that could be detrimental to counting.

Alpha Counting and Age Calculation

More than 90 alpha ages were determined in the course of this work. Alpha decay of the samples was counted in an Ortec 576A alpha spectrometer (ALSP) system for 3 to 7 days. The spectrometer measures energies in the range of 0 to 10 Mev. The average energies of isotopes relevant to this dating method all fall in the range of 4.0 to 5.7 Mev. They are as follows: ^{232}Th: 4.0 Mev, ^{238}U: 4.185 Mev, ^{230}Th: 4.666 Mev, ^{234}U: 4.754 Mev, ^{232}U: 5.3 Mev, ^{228}Th: 5.398 Mev, ^{224}Ra: 5.684. The deviation from the average energy of an isotope can be up to 0.1 Mev, and therefore the area of the peak, and not the height, is a function of the number of alpha decays. Background noise is periodically measured and corrected for.

Subsequent to counting, a 34 counter-channel envelope (0.1660 Mev) is selected for each peak. Counts in each envelope are summed and the counter background and neighboring peak tails are subtracted from these sums. Background noise comprises two components: fixed background caused by the natural radiation of the counter and cosmic rays striking the detector; and variable background caused by recoil nuclei present between the disc and the detector (radiation from accumulated particles released from previous samples). The most common recoil nuclei are those of the ^{232}U spike daughters, ^{228}Th, ^{224}Ra, and ^{220}Rn. Precise knowledge of this variable background is necessary when low-activity samples are measured. The background due to recoil differ for uranium and thorium sources, and therefore these were counted on separate detectors. Tails (T) of neighboring peaks must be subtracted from the peak sums according to the following equations (Kaufman, pers. comm.):

$T_{(230Th)}=0.002*{}^{228}Th$

$T_{(232Th)}=0.002*{}^{230}Th$

$T_{(228Th)}=0.093*^{224}Ra$

$T_{(234U)}=0.016*^{232}U$

$T_{(232U)}=0.047*^{224}Ra$

$T_{(238U)}=0.003*(^{234}U+(0.019*^{232}U))$

The ^{228}Th isotope, introduced as a spike, also occurs naturally in detritus, in an amount equal to the amount of ^{232}Th in the detritus and is accordingly corrected for.

The detrital non-carbonate component of the samples, indicated by the presence of ^{232}Th, was corrected for using ^{232}Th as an index of ^{230}Th contamination (as described in Kaufman et al, 1998). The Soreq Cave has a rigorously determined $^{230}Th/^{232}Th$ ratio of 1.8, while the crustal average is 3.8. Kaufman et al. (1998) recommend correction for samples with $^{230}Th/^{232}Th < 30$ or whereas others recommend correction for samples with $^{230}Th/^{232}Th < 20$ (Smart, 1991). The samples dated in this work showed a low degree of detrital contamination. 92% of samples showed $^{230}Th/^{232}Th > 20$; 88% had $^{230}Th/^{232}Th > 30$, and 67% had $^{230}Th/^{232}Th > 100$. Corrections were made for all samples with $^{230}Th/^{232}Th < 100$. In this study corrected ages are presented for all samples with $^{230}Th/^{232}Th$ ratio < 100, while the non-corrected ages are also available.

There are three types of error involved in dating that need to be taken into account. Analytical errors include human error, memory effects in analytical equipment (glassware and detectors), and contamination of reagents by U and Th, and failure to separate the U and Th thoroughly in chemical procedures. It should be noted that uncertainties in the concentration of spike solution or the amount of spike solution used do not affect age calculation, as long as spike isotopic ratios are unaffected. Analytical errors are almost always negligible compared to the statistical error.

Counting error (statistical error due to radioactive decay randomness) is the only error that is readily quantifiable. It is usually quoted as $\pm\sigma$ of the activity ratios (Ivanovich and Murray, 1992). Error for each isotope is calculated using the following equation:

$$\sigma N = \sqrt{N + backN + tailN}$$

while N is the number of counts, $backN$ is the number of background counts corrected for, and $tailN$ is the number of tail counts corrected for.

The error for the isotope ratios is given here:

$$\sigma\frac{N1}{N2}=\frac{N1}{N2}*\sqrt{\left(\frac{\sigma N1}{N1}\right)^2+\left(\frac{\sigma N2}{N2}\right)^2}$$

while N1 is the activity of one isotope and N2 is the activity of a second. The errors of $^{230}Th/^{234}U$ and $^{234}U/^{238}U$ determine the error of the age. The maximum age is calculated by using the highest $^{230}Th/^{234}U$ ratio and the lowest $^{234}U/^{238}U$ ratio, while the minimum age is calculated by using the lowest $^{230}Th/^{234}U$ ratio and the highest $^{234}U/^{238}U$ ratio.

Ages were calculated according to Kaufman and Broecker (1965):

$$\left(\frac{^{230}Th}{^{234}U}\right)_C=\left[\left(\frac{^{238}U}{^{234}U}\right)*\left(1-e^{-\lambda_{230}t}\right)\right]+\left[1-\left(\frac{^{238}U}{^{234}U}\right)_C\right]*\left(\frac{\lambda_{230}}{\lambda_{230}-\lambda_{234}}\right)*\left(1-e^{-(\lambda_{230}-\lambda_{234})t}\right)$$

using the Newton-Raphson iterative method described by Ivanovich and Murray (1992). This method consists of inserting trial values of t into the above equation and approaching a solution for t, which appears twice as an exponent in the equation. It is also possible to graphically determine the ages using a plot of $^{234}U/^{238}U$ versus $^{230}Th/^{234}U$ (Kaufman and Broecker, 1965). The decay constants used for calculations are $\lambda_{234}= 2.835*10^{-6}\ y^{-1}$ for ^{234}U and $\lambda_{230}= 9.195*10^{-6}\ y^{-1}$ for ^{230}Th (Kaufman et al., 1998).

Age determination by correlation with stable isotope profile

The absolute dating method available for this paleoseismic study was alpha spectrometry, which has accurate results, however the error is quite large (5-20%) and the amount of sample needed is substantial. A novel approach for improving the alpha - determined ages was used for the first time during this study, owing to the continuous stable isotope profile that exists for the Soreq Cave. All the samples of this work are from the Soreq Cave and from the near-by Har -Tuv Cave, which has nearly identical climatic and hydrological conditions. $\delta^{18}O$ and $\delta^{13}C$ were measured on samples from this study and their profiles were compared to those of Bar- Matthews et al. (1993, 1996, 1997, 1999, 2000a,b) and Kaufman et al. (1998) in the same age range. The range of $\delta^{18}O$ values in the Soreq Cave speleothems is –2.5 to –8.5 ‰ PDB and –1.75 to –13 ‰ PDB for the $\delta^{13}C$ values. These large oscillations allow us to straightforwardly correlate this study's profiles

with the existing one (Fig. 8). Since the Soreq Cave profile has been dated rigorously using the TIMS method this correlation method improves the ages of this work significantly, with an approximate error of 1-2%.

This method of determining age by comparing isotope profiles to a well-dated record is well known in deep sea cores as wiggle matching (e.g. Martinson et al, 1987; Hoek and Bohncke, 2001). Sapropel events were dated by wiggle-matching with the $\delta^{18}O$ record of the Soreq Cave because sapropels older than 10 ky could not be directly dated (Bar-Matthews et al., 2000a). In the current study, this is the first time that speleothems (and through them, tectonic events) are dated by correlation with a well-established stable isotope profile from other speleothems. It is all the more promising given that the speleothems are from the same cave or from a very nearby cave.

Isotope ratios of oxygen and carbon in speleothems are a source of diverse information about the past. They have been used extensively in paleoclimate studies worldwide (Thompson et al., 1976; Schwarcz, 1986; McDermott et al., 1999), in Israel (Issar et al., 1992; Frumkin et al., 1994, 1999), and specifically in the Soreq cave (Bar-Matthews et al., 1993, 1996, 1997, 1999, 2000a,b). The stable isotope profile for the Soreq Cave comprises 3800 measurements from 23 different speleothems from various locations within the cave (Bar-Matthews et al., 2000b). These samples have been dated extensively by the ^{230}Th-U dating method. Ninety-five age determinations were established by Thermal Ionization Mass Spectrometry (TIMS) according to the procedure described by Kaufman et al. (1998). A continuous record was assembled by comparing the records of several speleothems covering similar time intervals and excellent matches were found. TIMS dating was performed on consecutive lamina ~ 10 mm thick, whereas the carbon and oxygen isotopic measurements were carried out every ~ 0.5 mm. An assumption was made that the measured age represents the center of the lamina, and that the growth rate from the center to the margin of each lamina is constant. The isotopic record has no significant time intervals in which ages are absent and therefore it is considered essentially continuous.

The speleothems in this study were sampled every 0.5 mm using a diamond drill in order to obtain a very high resolution stable isotope record. The $\delta^{18}O$ and $\delta^{13}C$ values were plotted and compared to the Soreq Cave profile pertinent to the time range given by the alpha age. The sample closest to the collapse contact was identified and its age was determined by comparison with the Soreq Cave profile. The errors on these ages are small

for a number of reasons: the 0.5 mm diamond drill can drill very close to the contact without contamination of the sample; the small amount of material used generates an age closer to the true age of the collapse event than when a thicker lamina is used for alpha dating (which averages the range of ages included in the whole of the lamina); the profile is compared to the Soreq Cave profile which has been rigorously dated by TIMS at a high density.

Isotope measurements of $\delta^{18}O$ and $\delta^{13}C$ were performed on 0.2-0.5 mg of calcite. Phosphoric acid extraction was made at 90^0C. All $\delta^{18}O$ and $\delta^{13}C$ values were calibrated against the international standard NBS-19, and are reported in permil, relative to the Pee Dee Belemnite (PDB) standard. The standards used for comparison were NBS-19 and an internal Carrara marble standard. The carbonate powder was analyzed for $\delta^{18}O$ and $\delta^{13}C$ using a VG Isocarb system attached to a SIRA-II mass spectrometer.

TIMS

We chose three samples that gave very young α ages (HT-15A, HT-12A, and SO-38C) for dating by the TIMS method. Young alpha ages can be problematic because due to the small amount of Th, the statistics are less reliable. It is therefore beneficial to verify by comparison with TIMS ages. The samples were analyzed at the Geotop laboratories at the University of Quebec à Montreal, using the Lunatic I mass spectrometer. The advantage of the TIMS method is two-fold: the amount of sample needed is small compared to the necessary amount for α–counting, and the error is minor (0.5-1% of the age) in comparison to the α–method (5-10%). TIMS dating of more samples would improve this record and corroborate our wiggle-matching age determination.

5. Results and discussion

Maps of the Soreq and Har-Tuv Caves were prepared, which present fracture orientations (Fig. 3, Fig. 4) and collapse sites. Collapsed blocks and cave deposits were described and mapped and show preferred EW orientation (Fig. 7). This preferred orientation supports the working hypothesis of earthquake-induced collapse. Samples were taken as described above and alpha dating was performed on pre and post collapse lamina.

More than 90 alpha ages were determined in the course of this work (Table 1). Ages range from very recent (<100 years) to older than the method limit (~>300 ky). The error is presented as plus and minus (ky) and also as a percentage of the age, and usually ranges from ~ 4% to 10% for samples younger than 200 ky. The significant isotope ratios presented are: $^{234}U/^{238}U$ (R48), $^{230}Th/^{232}Th$ (R02), and $^{230}Th/^{234}U$ (R04). TIMS dating on three samples and duplicate alpha measurements on a number of samples express the reliability of the ages. The concentrations of U and Th measured by alpha counting and by ICP measurement are given. These values should be similar, as an indication of reliability. When not compatible, one of the measurements was duplicated. Chemical yields are for the most part very good. All alpha measurements performed are given here, including pre contact, post-contact, and other pertinent speleothem lamina.

Table 2 presents in chronological order the age of collapse events, determined by the "stable isotope correlation method" described above. Alpha and TIMS ages are shown as well. Maximum ages represent the last lamina to grow before collapse, while minimum ages represent the first lamina to grow after collapse. An ideal collapse for dating would provide a minimum and maximum age (pre -collapse and post- collapse); however this situation does not always exist. More than 40 collapses were dated, and we determined 19 separate collapse ages. Nine collapses were dated to the past 20 ky, which group into 5 to 6 separate collapse events (Fig. 9). Only one of these was found in the Soreq Cave, and it is important to determine whether this is a sampling bias or due to the fact that recent earthquakes have had a larger effect on the shallower (and perhaps more susceptible) Har-Tuv Cave. In the time period between 20 and 80 ky we dated 8 collapses, which show 6 collapse events (Fig. 10). In the time between 80 ky and 160 ky we have dated 12 collapses, which represent 7 collapses events (Fig. 11). Twelve collapses were found to be older than the alpha-counting method limit.

An example of the correlation between the stable isotope profile of one sample from this study and of the Soreq Cave profile is given in Fig. 6. All dated samples are plotted with the Soreq Cave isotopic profile in Fig. 8.

As further corroboration for the collapses being earthquake-induced, we anticipated finding more than one collapse that occurred at the same time. The results show that at least 5 of the collapse ages were found more than once, while 2 of these events are documented in both caves.

6. Correlation with other paleoseismic studies

This study presents a large number of dated collapsed speleothems and ceiling blocks. The majority of collapses can be correlated with earthquakes discovered in other paleoseismic works. The ages of collapses events show no association with major climatic events (for example from glacial to interglacial; 19 to 16 ky or 135 to125 ky) and therefore we can construe that the ages are of tectonic events. The preliminary interpretations and correlations introduced here show that this method of using seismically disturbed cave deposits to date earthquakes is feasible and correlateable. Further sampling and dating can improve collapse ages that are not well established and may verify the completeness of this record. Since it is thought that earthquakes affect the underground at a lesser intensity, these dated earthquakes may represent very large seismic events, and may allow the evaluation of recurrence rates for very large earthquakes.

Correlation with historical earthquakes and recently deformed Dead Sea sediments

The historical earthquake record of the last 4 millennia in the Middle East is one of the longest historical seismic records in existence (Ben-Menahem, 1991). Extensive geological investigation of this period supports this record (Reches & Hoexter, 1981; Niemi and Ben-Avraham, 1994; Migowski et al., 1999; Enzel et al., 2000; Klinger et al., 2000; Ken-Tor et al., 2001; Migowski, in prep).

The collapses dated from 20 ky to the present are shown in Fig. 9. The number of collapses dated for each time period is shown along with possible correlations with historically and geologically documented seismic events. No other paleoseismic work deals with the time period of the two collapses that occurred at ~13 ky.

Correlation with deformed Lisan Formation layers

Until the present study, the 50,000-year paleoseismic record (70-20 ky BP) recovered in the laminated sediments of the Lisan Fm. (Marco and Agnon, 1995; Marco et al., 1996) was the sole recorder of this period, with regard to earthquakes. The current study covers this time period, and reveals a number of earthquakes that can be correlated with the dated mixed layers of the Lisan Fm. Distribution of the dated collapses in the time period between 80 and 20 ky, is exhibited in Fig.10. Collapse events G through K have been found in one location each, while L has been dated in two locations in the Soreq Cave. Ages of collapses G, H, and L are well constrained, because pre-collapse and post-collapse lamina were available for dating. All collapses except K can be correlated with mixed layers from the Perazim Valley section (Marco et al., 1996). The relatively large thickness of the 52.1 and 44.2 ky mixed layers (48 cm and 37 cm, respectively) supports the suggestion that large collapses occurred in the Soreq and Har-Tuv Caves. The analytical error for purely aragonite Lisan samples, dated by the TIMS U-Th method, is <1%, however the ages may be slightly younger due to detrital contamination (Marco et al., 1996). Further error may exist in the ages of the mixed layers as a result of the assumption that sedimentation rates are bimodal and constant. However, the mixed layers correlative with G, J, and L collapses have well constrained ages due to the fact that they are very near lamina with absolute ages. Further investigation into these correlations will be carried out using new evidence concerning ages of the Lisan Fm. (Schramm et al., 2000).

Collapses older than the Lisan Fm. represent the only paleoseismic record of its age in the region (Fig. 11). In this period 3 groups of collapses are observed: 2 collapses occurred at ~107 ky (O), 2 collapses at the Soreq Cave occurred at ~128 ky (P), and 4 collapses at the Har-Tuv and Soreq caves occurred at ~144 ky (R). Future work on the mixed layers of the Samra Fm., in the Dead Sea Rift Zone, may produce a record correlateable with ours. Twelve collapses were dated to be older than the 185 ky correlation limit, 8 of them are older than the alpha method limit (~300 ky).

7. Future Plan

There is a need to date more collapses in the Soreq Cave, in order to investigate the fact that to date we have found only one young (<12 ky) collapse there. Is this a sampling bias, or have recent earthquakes had a lesser local intensity than in the past, and therefore have only caused collapses in the shallower Har-Tuv Cave? We plan to further interpret and refine our results. More dated collapses will aid us in attempting to interpret cyclicity of earthquakes. We will try to establish ages of opening and closing of cracks in the caves by dating beginning and ending of growth of speleothems and we will attempt correlation with tectonic events. The isotopic profile of each sample will be presented (as in Fig. 6) together with the Soreq Cave stable isotope record for that period. Maps of the study caves, including location and age of the collapses, will be presented. Interpretation regarding the exact location of the collapses in the caves will be attempted. Schematic diagrams of demonstrative collapses and regrowths will be prepared.

We plan to extend this research to the Galilee in order to examine the long-term seismic behavior of Northern Israel. The Ga'aton Cave will be one focus of this research, due to the fact that it has an enormous amount of speleothem and ceiling collapses, covered by post-collapse regrowth. The paleoseismic record in the cave will possibly be correlateable with other seismic events in Northern Israel (e.g. Ellenblum et al., 1998; Gluck, 2001).

Along the Rosh Pina Bypass Road there are a number of open fractures filled with speleothems. Arkin (1996) relates these fractures to Dead Sea Transform tectonic events. Dating of these deposits may give insight into the timing and nature of these fractures.

References

Ambraseys, N.N., Melville, C.P., Adams, R.D., 1994. Macroseismic information. The seismicity of Egypt, Arabia, and the Red Sea- a historical review. *Cambridge University Press,* 19-110.

Amiran, D.H.K., Arieh, E., Turcotte, T., 1994. Earthquakes in Israel and adjacent areas; macro seismic observations since 100 B.C.E. *Israel Exploration Jour.*, 44,260-305.

Amit, R., Zilberman, E., Enzel, Y., Porat, N., 1996. Young faults and earthquake risk in the Elat area: field trip to the fault systems of Nahal Shehoret and Melehat Avrona. *Isr. Geol. Soc. Ann. Meeting, Field Trips.* 1-21.

Amit, R., Zilberman, E., Porat, N., Enzel, Y., 1999. Relief Inversion in the Avrona Playa as evidence of large-magnitude historical earthquakes, southern Arava Valley, Dead Sea Rift. *Quat. Res.* 5,1,76-91.

Arkin, Y., 1980. Survey of karstic phenomena in the western Judean Hills. *Isr. Geol. Surv.*, Rep.80/5/m.m. (in Hebrew).

Arkin, Y., 1996. Fractures and karst in hard carbonates in Northern Israel. *Geol. Surv. Isr. Current Research.* 10, 90-94.

Arkin, Y., Braun, M., Starinsky, A., 1965. Sections of Cretaceous formations in the Jerusalem-Beit Shemesh area, lithostratigraphy. *GSI, Jerusalem,* Pub. No.1.

Asaf, M., 1975. Karstic phenomena in the Soreq Cave. *M.Sc.thesis, Tel Aviv Univ.*, Tel Aviv, (in Hebrew).

Avni, R., 1999. The 1927 Jericho earthquake, comprehensive macroseismic analysis based on contemporary sources. *Ph.D. thesis, Ben-Gurion University of the Negev.* (in Hebrew, English abstr.)

Ayalon, A., Bar-Matthews, M., Kaufman, A., 1999. Petrography, strontium, barium and uranium concentrations, and strontium and uranium isotope ratios in speleothems as paleoclimatic proxies: Soreq Cave, Israel. *The Holocene*, 9.6, 715-722.

Bar-Matthews, M., Ayalon, A., Kaufman, A., 1997. Late Quaternary paleoclimate in the Eastern Mediterranean region from stable isotope analysis of speleothems at Soreq Cave, Israel. *Quat. Res.*, 47, 155-168.

Bar-Matthews, M., Ayalon, A., Kaufman, A., 2000a. Timing and hydrological conditions of sapropel events in the Eastern Mediterranean, as evident from speleothems, Soreq cave, Israel. *Chem. Geol.*, 169,145-156.

Bar-Matthews, M., Ayalon, A., Kaufman, A., Wasserburg, G.J., 1999. The Eastern Mediterranean paleoclimate as a reflection of regional events: Soreq Cave, Israel. *Earth Planet. Sci. Lett.*, 166, 85-95.

Bar-Matthews, M., Ayalon, A., Matthews, A., Frumkin, A., 2000b. Eastern Mediterranean paleoclimate during the last 250, 000 years as derived from the petrography, mineralogy, trace element and isotopic composition of cave deposits (speleothems), Israel. *Geol. Surv. Isr. Report.* TR-GSI/10/2000.

Bar-Matthews, M., Ayalon, A., Matthews, A., Halicz, L., Sass, E., 1993. The Soreq Cave speleothems as indicators of paleoclimate variations. *Geol. Surv. Isr. Current Research*, 8, 1-3.

Bath, M., 1973. Introduction to Seismology. *Birkenhauser* 395 p.

Ben-Menahem, A., 1991. Four thousand years of seismicity along the Dead Sea rift. *J. Geophys. Res.* 96, B-12, 20 195-20 216.

Chen, J. H., Wasserburg, G. J., Curran, H, A., White, B., 1990. ^{234}U and ^{230}Th in groundwaters and ^{230}Th ages of fossil corals. *E.O.S.*, 71, 1719.

Crispim, J. A., 1999. Seismotectonic versus man-induced morphological changes in a cave on the Arrabida chain (Portugal). *Geodinamica Acta,* 12, 3-4, 135-142.

Disni, 1997. Map of Yaala Cave. Unpublished data of the Center for Cave Research, Israel.

Edwards, R. J., Chen, J. H., Wasserburg, G. J., 1987. ^{238}U-^{234}U-^{230}Th-^{232}Th systematics and the precise measurement of time over the past 500,000 years. *Earth Planet, Sci. Lett.*, 81, 175-192.

Eisenstein, B., 1970. Hartuv cave- geological engineering report. *Tahal Engineering Consultants Inc.*, (in Hebrew).

Ellenblum, R., Marco, S., Agnon, A., Rockwell, T., Boas, A., 1998. A crusader castle torn apart by the earthquake of dawn, 20 May 1202. *Geology*, 26, 303-306.

Enzel, Y., Amit, R., Porat, N., Zilberman, E., Harrison, B. J., 1996. Estimating the ages of fault scarps in the Arava, Israel. *Tectonophysics*, 253, 305-317.

Enzel, Y., Kadan, G., Eyal, Y., 2000. Holocene earthquakes inferred from a fan-delta sequence in the Dead Sea graben. *Quat. Res.* 53,1, 34-48.

Even, H., 1983. The variation of chemical and isotopic composition of karst water in the upper vadose zone in the Judean Hills. *M.Sc. thesis, Hebrew University of Jerusalem.* (in Hebrew, English abstr.).

Fink, M., 1962. Geology of the Hartuv-Shaar Hagay area. *M.Sc. thesis, Hebrew University of Jerusalem* (in Hebrew).

Forti, P., 1998. Seismotectonic and paleoseismic studies from speleothems: the state of the art. *Han 98-Tectonique, karst et seismes*, 79-81.

Forti, P., Postpischl, D., 1984. Seismotectonic and paleoseismic analyses using karst sediments. *Marine Geol.*, 55, 145-161.

Frumkin, A., Ford, D. C., Schwarcz, H. P., 1999. Continental oxygen isotope record of the last 170, 000 years in Jerusalem. *Quat. Res,* 51, 317-327.

Frumkin, A., Schwarcz, H.P., Ford, D., 1994. Evidence for isotopic equilibrium in stalagmites from caves in a dry region: Jerusalem, Israel. *Isr. J. Earth Sci.*, 43: 221-230.

Gascoyne, M., Schwarcz, H.P., Ford, D.C., 1978. Uranium-series dating and stable isotope studies of speleothems: Part I theory and techniques. *Brit. Cave Res. Assoc.* Vol. 5 (2).

Gilli, E., 1999a. Evidence of paleoseismicity in a flowstone of the Observatoire cave (Monaco). *Geodinamica Acta,* 12, 3-4, 159-168.

Gilli, E., 1999b. Rupture de speleothemes par fluage d'un remplissage endokarstique. L'example de la grotte de Ribiere (Bouches-du-Rhone). *C.R. Acad. Sci. Paris, Science de la terre et des planetes*, 329, 807-813.

Gilli, E., Levret, A., Sollogoub, P., Delange P., 1999. Research on the February 18, 1996 earthquake in the caves of the Saint-Paul-de-Fenouillet area, (eastern Pyrenees, France). *Geodinamica Acta*, 12, 3-4, 143-158.

Gluck, D., 2001. Unpublished MSc. (in Hebrew). Hebrew Univerity of Jerusalem.

Guidoboni, E., Comastri, A., Traina, G., 1994. Catalogue of ancient earthquakes in the Mediterranean area up to the 10th century. *Instituto Nazionale di Geofisica, Roma.* 504.

Halicz, L., Bar-Matthews, M., Ayalon, A., Kaufman, A., 1997. Determination of low concentrations of U and Th in carbonate rocks using FHCP-MS. *Atomic Spectroscopy.* 18, 6, 175-179.

Hoek, W. Z., and Bohncke, S. J. P., 2001. Oxygen-isotope wiggle matching as a tool for synchronizing ice-core and terrestrial records over Termination 1. *Quat. Sci. Rev.* 20, 1251-1264.

Issar, A. S., Govrin, Y., Geyh, M. E., Wakshal, E., Wolf, M., 1992. Climate changes during the Upper Holocene. *Israel. Isr. J. Earth Sci.* 40, 219-223.

Ivanovich, M., and Harmon, R. S., eds., 1992, Uranium-series disequilibrium, Applications to earth, marine, and environmental sciences, 2nd edition, Oxford University Press.

Jibson, R. W., 1996. In: McAlpin (editor), *Paleoseismology*. Academic Press, London.

Kaufman, A., Broecker, W., 1965. Comparison of ^{230}Th and ^{14}C ages for carbonate materials from lakes Lahontan and Bonneville. *J. Geophys. R.* Vol. 70, No. 16, 4039-4054.

Kaufman, A., Wasserburg, G.J., Porcelli, D., Bar-Matthews, M., Ayalon, A., Halicz, L., 1998. U-Th isotope systematics from the Soreq Cave, Israel and climatic correlations. *Earth Planet, Sci. Lett.,* 156.

Ken-Tor, R., Agnon, A., Enzel, Y., Stein, M., Marco, S., Negendank, J.F.W., (2001). High-resolution geological record of historic earthquakes in the Dead Sea basin. *J. Geophys. Res.*106, B2, 2221-2234.

Klinger, Y., Avouac, J. P., Dorbath, L., Abou Karaki, N., Tisnerat, N., 2000. Seismic behavior of the Dead Sea fault along Araba Valley. *Geophys. J. Int.* 142, 769-782.

Lally, A. E., 1992. Chemical Procedures. In: Ivanovich, M., and Harmon, R. S., eds. *Uranium-series disequilibrium, Applications to earth, marine, and environmental sciences.* 2nd edition, Oxford University Press, 95-126.

Lasman, N., 1965. Geological report on the Hartuv Quarry for Hartuv Quarries Ltd. *Geol. Surv. Mineral Resources Dept.* Report No. M.P. 156/65.

Lemeille, F., Cushing, M., Carbon, D., Grellet, B., Bitterli, T., Flehoc, C., Innocent, C., 1999. Co-seismic ruptures and deformations recorded by speleothems in the epicentral zone of the Basel earthquake. *Geodinam. Acta*, 12, 3-4, 179-191.

Marco, S., Agnon, A., 1995. Prehistoric earthquake deformations near Massada, the Dead Sea graben. *Geology,* 23, 695-698.

Marco, S., Stein, M., Agnon, A., Ron, H., 1996. Long-term earthquake clustering: A 50,000 year paleoseismic record in the Dead Sea Graben. *J. Geophys. R.*, 101, 6179-6191.

Martinson, D. G., Pisias, N. G., Hays, J. D., Imbrie, J., Moore, T. C. Jr., Shackleton, N. J., 1987. Age dating and the orbital theory of the ice ages: development of a high-resolution 0 to 300,000-year chronostratigraphy. *Quat. Res.*27, 1-29.

McCalpin, J. (Editor), 1996. Paleoseismology. *Academic Press*, London.

McDermott, F., Frisia, S., Huang, Y., Longinelli, A., Spiro, B., Heaton, T.H.E., Hawkesworth, C.J., Borsato, A., Keppens, E., Fairchild, I.J., van der Borg, K, Verheyden, S., Selmo, E., 1999. Holocene climate variability in Europe: evidence from $\delta^{18}O$, textural and extension-rate variations in three speleothems . *Quat. Sci. Rev.*, 18, 1021-1038.

Migowski, C., in submission. PhD, Potsdam University.

Migowski, C., Ken-Tor, R., Negendank, J. F. W., Stein, M., Mingram, J., 1999. Post-Lisan record documented in sediment sequences from the western shore area and the central basin of the Dead Sea, paper presented at Terra Nostra 98/6: 3rd ELDP Workshop, sponsor, Ptolemais, Greece.

Morinaga, H., Yonezawa, T., Adachi, Y., Inokuchi, H., Goto, H., Yaskawa, K., 1994. The possibility of inferring paleoseismicity from the paleomagnetic dating of speleothems, western Japan. *Tectonophysics*, 230, 241-248.

Niemi, T.M., and Ben-Avraham, Z., 1994. Evidence for Jericho earthquakes from slumped sediments of the Jordan River delta in the Dead Sea. *Geology*, 22, 395-398.

Postpischl, D., Agostini, S., Forti, P., Quinif, Y., 1991. Paleoseismicity from karst sediments: the "Grotta del Cervo" cave case study (Central Italy). *Tectonophysics*, 193, 3344.

Reches, Z., Hoexter, D. F., 1981. Holocene seismic and tectonic activity in the Dead Sea area. *Tectonophysics*, 80, 235-254.

Rotstein, Y., 1987. Gaussian probability estimate for large earthquake occurrence in the Jordan Valley, Dead Sea Rift. *Tectonophysics*, 141, 95-105.

Salamon, A., Hofstetter, A., Garfunkel, Z., Ron, H., 1996. Seismicity of the eastern Mediterranean region: Perspective from the Sinai subplate. *Tectonophysics*, 263, 293-305.

Schramm, A., Stein, M, Goldstein, S., 2000. Calibration of the ^{14}C time scale to >40 ka by ^{234}U-^{230}Th dating of Lake Lisan sediments (last glacial Dead Sea). *EPSL.* 175, 2740.

Schwarcz, H.P., 1986. Geochronology and isotopic geochemistry of speleothems. In: Fritz, P., Fontes, J.C., eds. *Handbook of environmental isotope geochemistry*. Vol 2. Elsevier, Amsterdam, 271-300.

Shrir, M., Shrir, A.R., 1969. Map of Soreq Cave, 1:100. For Nature Reserves Authority. 60/1612/2 m.s.

Smart P.L., 1991, Uranium-series dating. In: P.L. Smart and P.D. Francis (Editors), *Quaternary Dating Methods- a User's Guide*. Quat. Res. Assoc. Tech. Guide. 4, London, 45-83.

Thompson, P., Schwarcz, H. P., Ford, D. C., 1975. Stable isotope geochemistry, geothermometry, and geochronology of speleothems from West Virginia. *Geol. Soc. Am. Bull.* 87, 1730-1738.

Yeats, R.S., Sieh, K., Allen, C. R., 1997. *The Geology of Earthquakes*. Oxford University Press, New York.

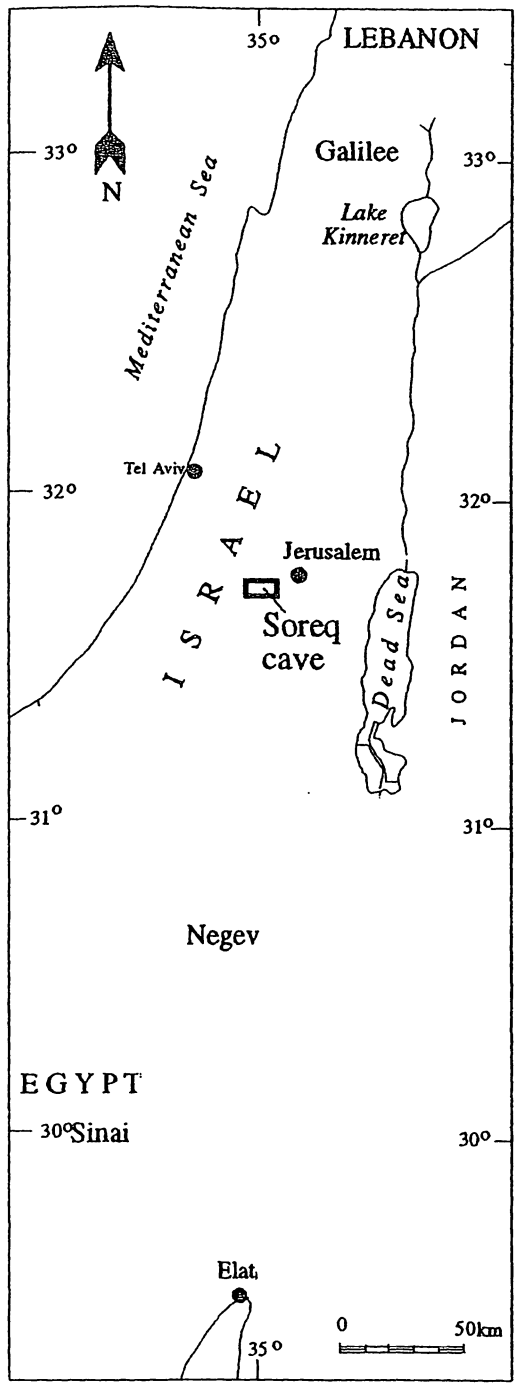

Fig. 1. Location of Soreq Cave. Har-Tuv Cave is in close proximity to Soreq

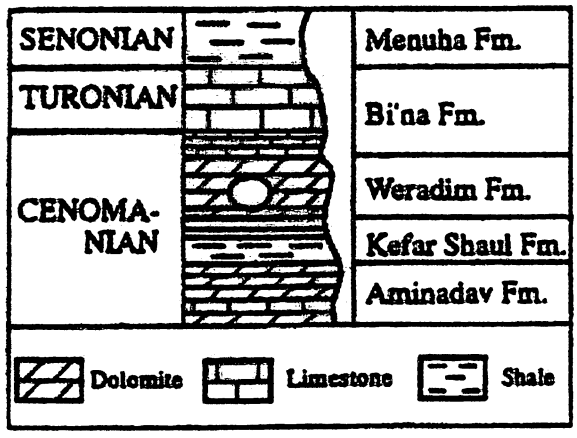

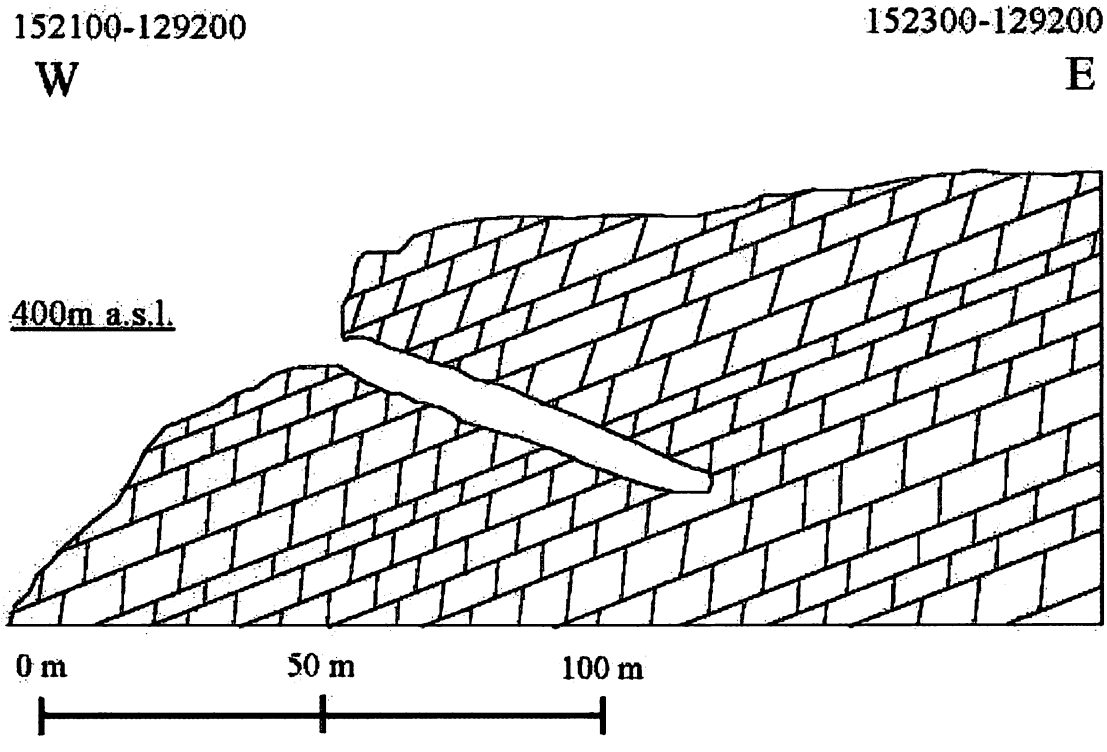

Fig.2. Schematic section of Soreq Cave showing the stratigraphic position of the cave (inset) in the dolomitic Weradim Formation.

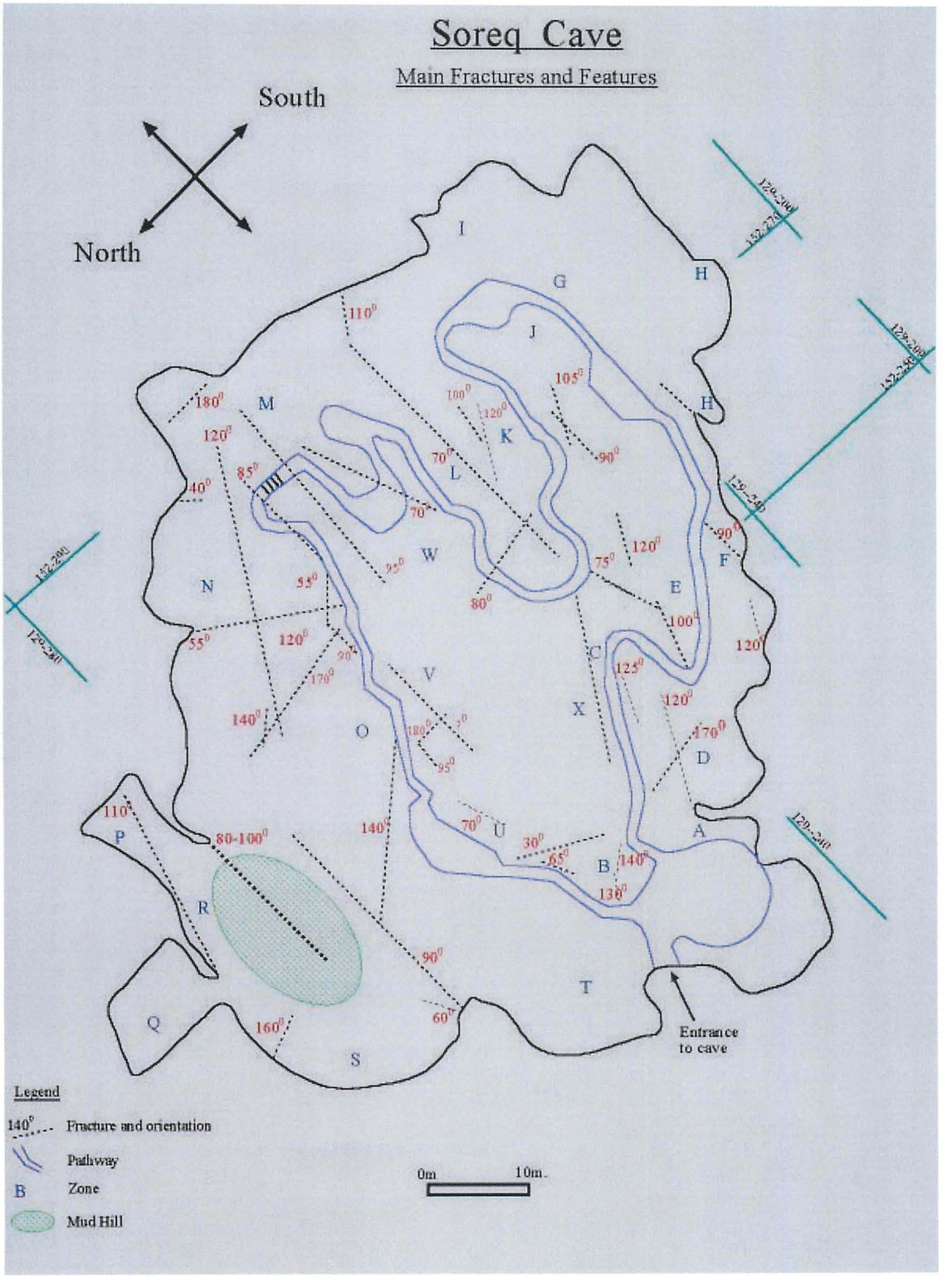

Fig. 3. Map of Soreq Cave, with fracture orientation marked.

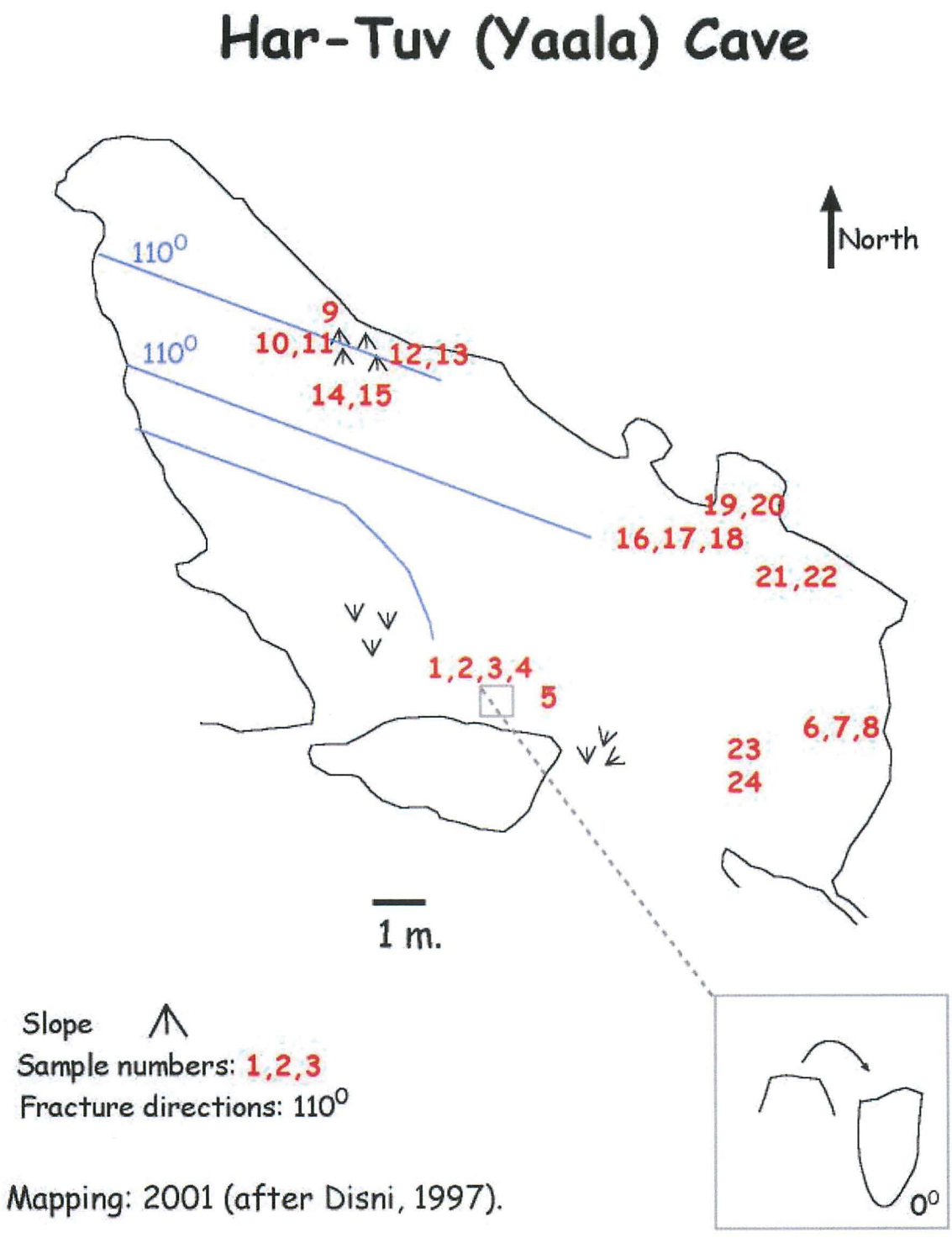

Fig. 4. Har-Tuv Cave. Collapse sampling locations are marked.

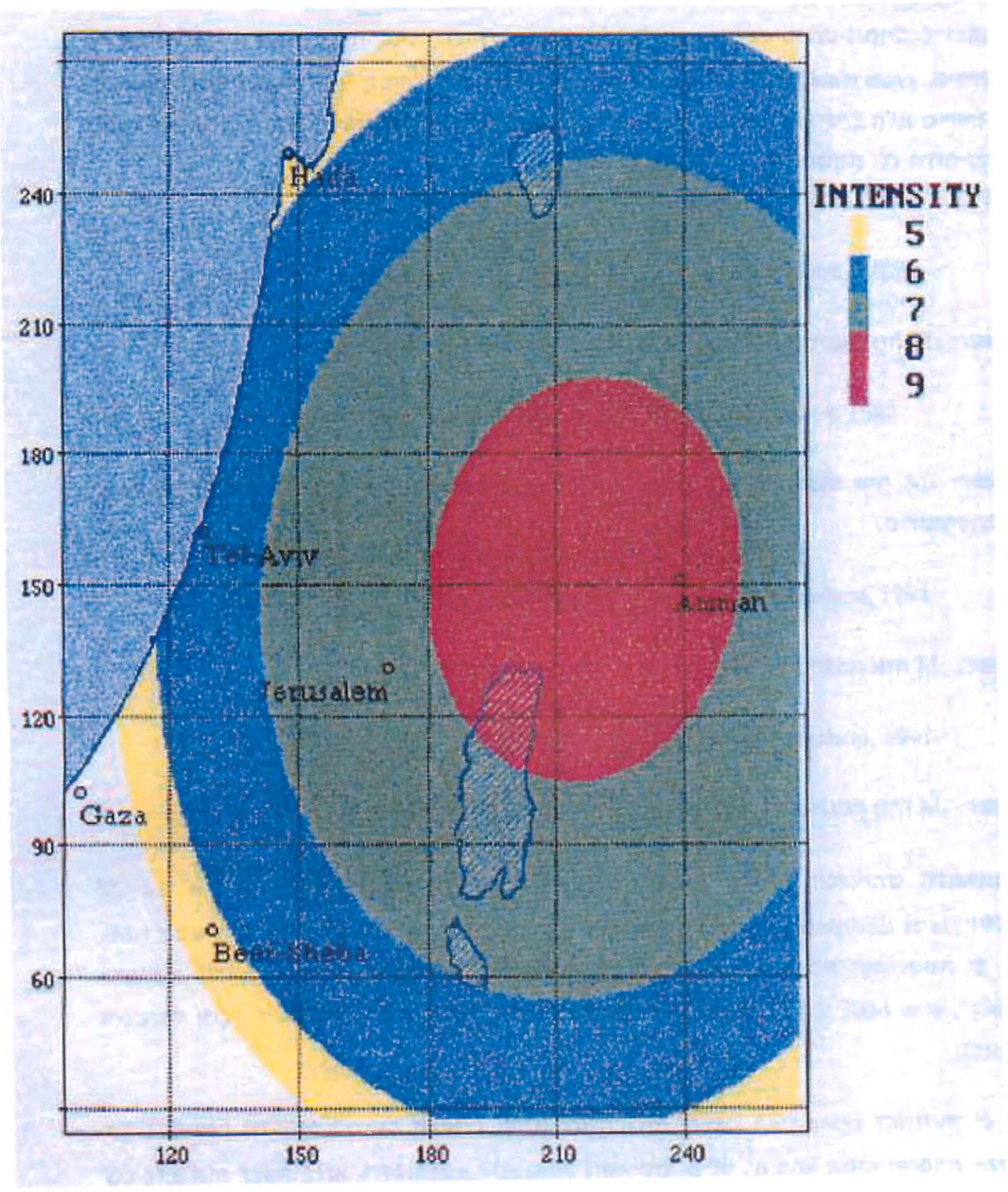

Fig. 5. Intensity map of the 1927 earthquake in the northern Dead Sea (Avni, 1999). The Soreq and Har-Tuv Caves, like Jerusalem, are in the intensity level VII area.

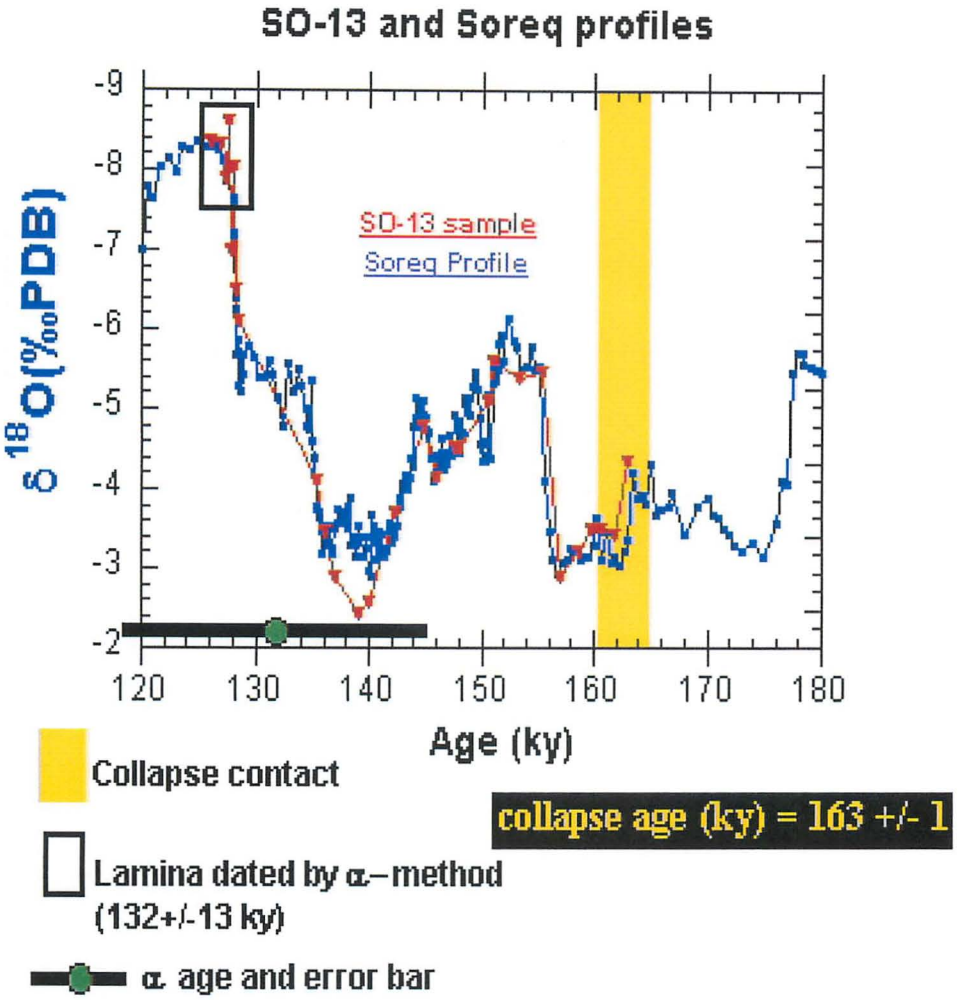

Fig.6. Oxygen isotope profile of collapse SO-13 superimposed on Soreq Cave profile. Alpha age and error of dated lamina shown. Yellow bar marks the collapse contact and the desired point for age determination.

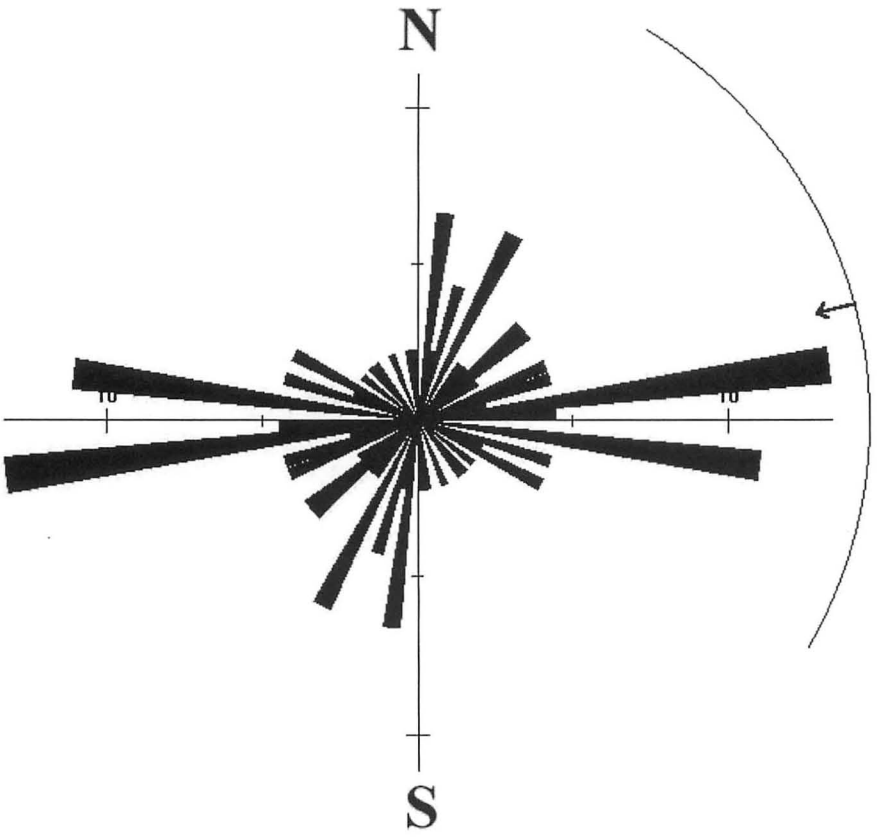

Fig.7. Orientation diagram of collapsed large (> 0.3 m) speleothems showing dominant EW orientations.

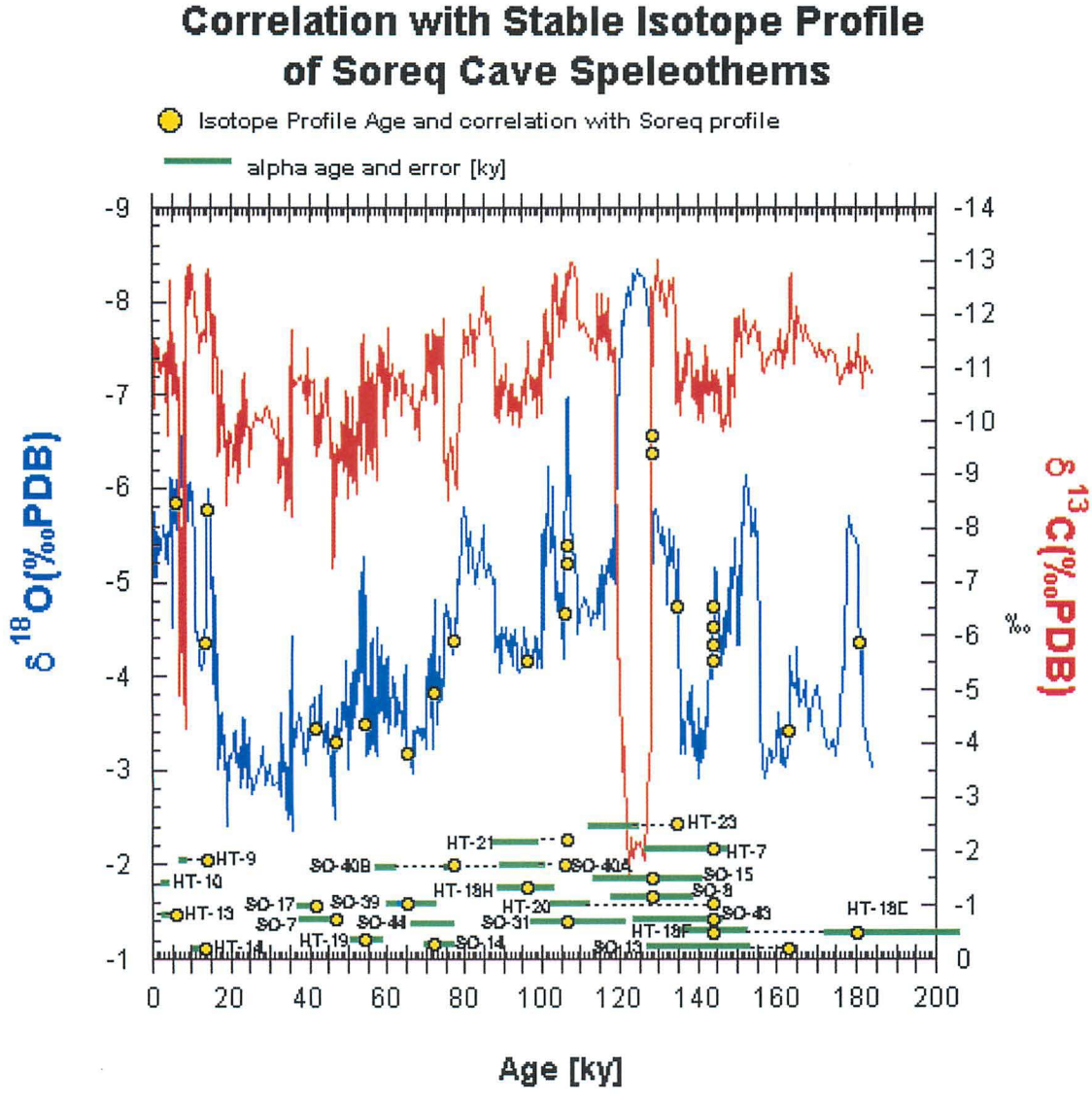

Fig. 8. Soreq Cave $\delta^{18}O$ (blue) and $\delta^{13}C$ (red) stable isotope profiles. Alpha ages with errors (green bars) and ages determined by stable isotope correlation from this study (yellow circles) superimposed.

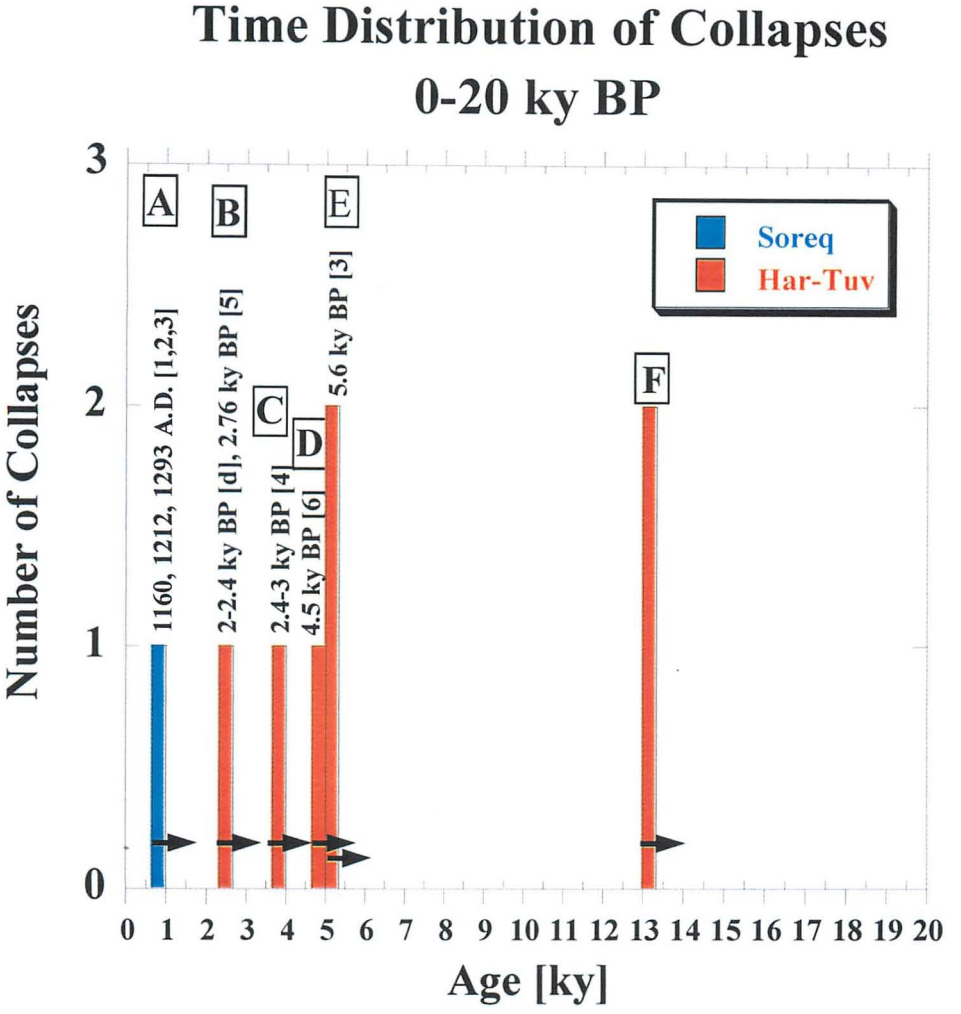

Fig. 9. Distribution of dated collapses in the past 20 ky years. Blue bars represent collapses in the Soreq Cave. Orange bars represent collapses in the Har-Tuv Cave. Arrows pointing to the right indicate collapses for which minimum ages were determined for. Historically and geologically documented earthquakes are marked above bars. References are given in square parentheses: [1] Amiran et al, 1994; [2] Ken-Tor et al., 2001; [3] Migowski, in preparation; [4] Enzel et al., 2000; [5] Ben-Menahem, 1991; [6] Gluck, 2001.

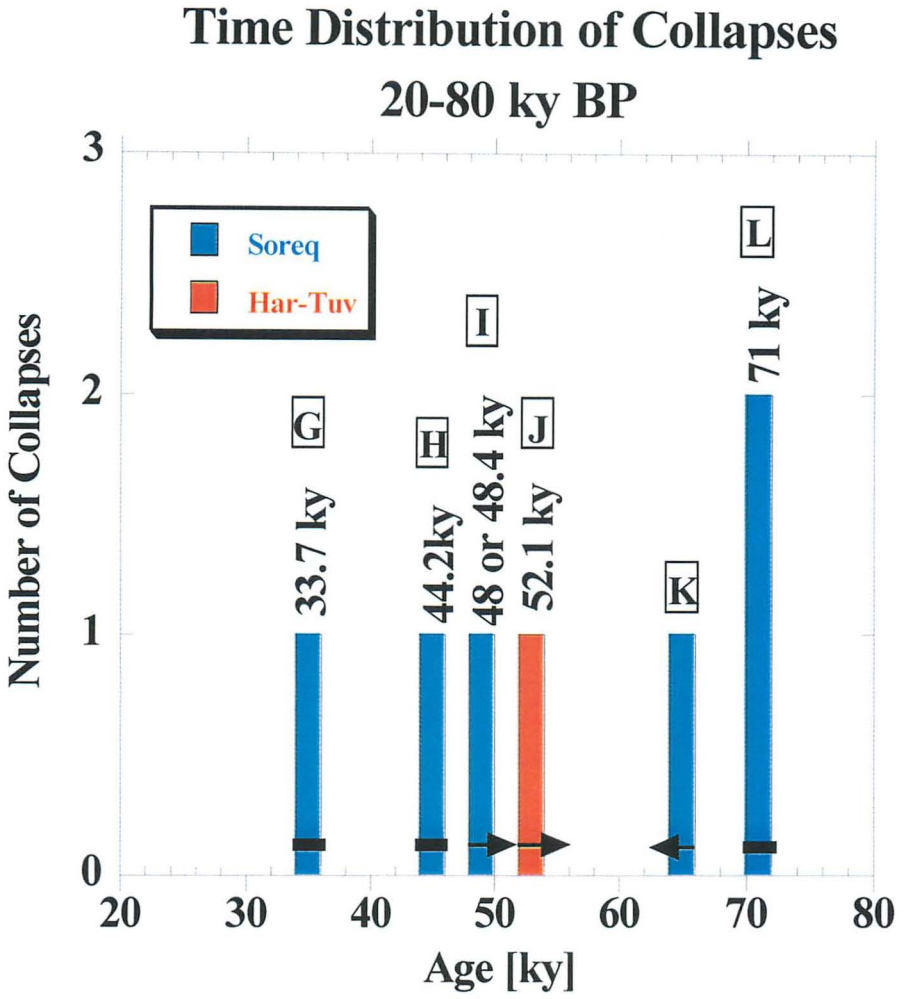

Fig. 10. Distribution of dated collapses in time, from 80 ky to 20 ky. Blue bars represent collapses in the Soreq Cave. Orange bars represent collapses in the Har-Tuv Cave. Arrows pointing to the right indicate collapses that minimum ages were determined for. Arrows pointing to the left indicate collapses that maximum ages were determined for. Black bars represent collapses that both minimum and maximum ages were determined for, greatly confining the age of collapse. Above bars are ages of mixed layers inthe Perazim section of the Lisan Fm (Marco et al., 1996).

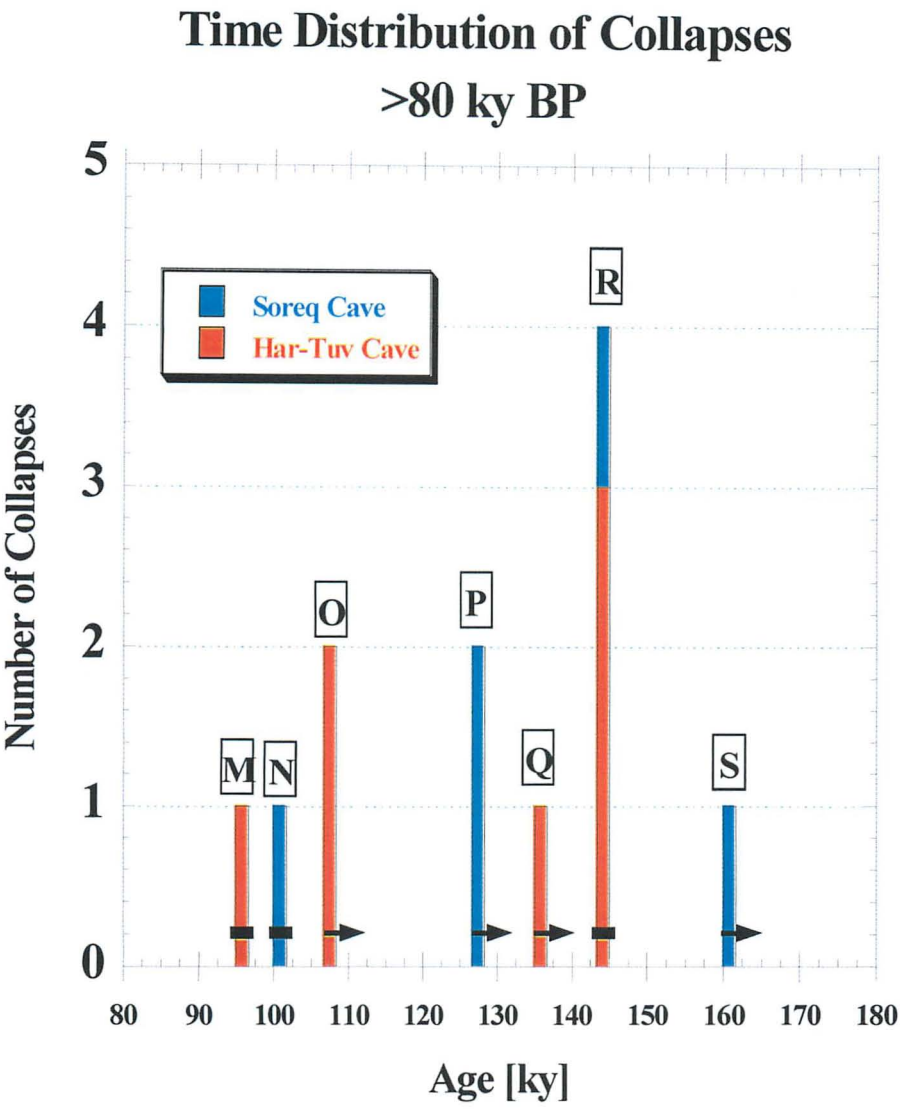

Fig. 11. Distribution in the time range of 180- 80 ky. Blue bars represent collapses in the Soreq Cave. Orange bars represent collapses in the Har-Tuv Cave. Arrows pointing to the right symbolize collapses that minimum ages were determined for. Black bars represent collapses that both minimum and maximum ages were determined for, greatly confining the age of collapse. No other paleoseismic study in Israel exists for this time period, and therefore no correlation is possible.

Table 1. U-Th analytical Results

Lab	Series	sample	Uicp ppb	U-a ppb	Thicp ppb	Th-a ppb	234U/238U	230T/234U	230T/232T	Yld-U	Yld-Th%	AGE ky	error+ ky	error- ky	% error	correction
*50	A	SO-3A		678.7		9.7	1.047	0.927	200.1	33	23	**268.1**	59	37	22	uncorrected
*50	C	SO-3E		241.3		1.7	1.063	0.894	44.8	32	38	**230.7**	75	41	32	corrected
*50	D	SO-6G		362.1		1.7	1.234	0.079	61.4	37	35	**8.9**	1	1	8	corrected
*51	A	SO-6A		658.8		-0.2	0.991	1.010	5581.1	39	31	**>method**				uncorrected
*51	B	SO-4D		171.5		11.3	1.120	0.659	33.5	45	15	**111.4**	15	13	14	corrected
*51	C	SO-3D		175.3		5.0	0.889	0.850	2.8	31	35	**>138**				corrected
*51	D	SO-2A		378.5		5.0	1.081	0.604	144.6	16	43	**99.1**	9	8	9	uncorrected
*52	A	SO-4A		8.6		5.1	1.047	0.847	189.2	34	17	**197.8**	31	23		uncorrected
*52	B	SO-4C		6.9		15.0	1.115	0.636	38.4	33	40	**107.3**	7	7		corrected
*52	C	SO-3C		9.1		26.3	1.015	0.983	58.8	28	14	**>309**				corrected
*52	D	SO-6C		25.5		4.9	1.144	0.512	466.4	29	30	**76.7**	3	3		uncorrected
*57	A	SO-9A	260.0	230.8	<10	1.3	1.025	0.993	521.7	43	54	**>313**				uncorrected
*57	B	SO-10A	226.0	197.2	2.5	8.3	1.050	1.026	75.6	45	17	**>324**				corrected
*57	C	SO-14A	677.0	584.9	28.6	2.3	1.119	0.498	419.0	54	31	**73.6**	3	3	5	uncorrected
*57	D	SO-15A	292.0	251.1	3.8	1.6	1.128	0.711	368.3	29	45	**130.1**	11	10	9	uncorrected
58*	A	S0-8A		434.0		5.1	1.019	0.707	181.6	42	14	**132.5**	13	11	9	uncorrected
58*	B	SO-8B	320.0	275.0	<10	8.6	1.028	0.672	65.4	17	36	**120.3**	11	9	8	corrected
58*	C	SO-8C		160.7		1.6	1.056	0.583	184.3	61	41	**94.2**	6	6	6	uncorrected
58*	D	SO-8D	300.0	319.6	<10	2.2	0.994	0.356	149.1	8	34	**47.9**	3	3	7	uncorrected
*59	A	SO-12C	890.0	784.0	<10	1.2	1.049	0.392	817.1	12	60	**53.8**	3	3	6	uncorrected
*59	B	SO-7A		548.1		13.7	1.068	0.347	44.8	18	29	**46.0**	3	3	7	corrected
*59	C	SO-7C		382.9		3.7	1.004	0.367	111.5	17	53	**49.8**	4	3	7	uncorrected
*59	D	SO-7D		346.5		0.4	1.074	0.315	897.6	8	60	**41.0**	4	3	9	uncorrected
*60	A	SO-16C	403.0	394.4	1.6	0.9	1.061	0.580	769.5	48	52	**93.3**	4	4	4	uncorrected
*60	B	SO-12B		637.0		97.7	1.128	0.418	10.0	48	3	**58.1**	7	6	11	corrected
*60	C	SO-12A		490.0		-0.2	1.118	0.546	341.2	35	12	**84.3**	6	6	7	uncorrected
*60	D	SO-16A		479.2		-0.2	1.089	0.564	1647.0	32	15	**89.0**	6	5	6	uncorrected
*61	A	SO-16D		468.7		2.4	1.031	0.502	293.0	38	31	**75.5**	4	4	5	uncorrected
*61	B	SO-13B		262.6		6.6	1.066	0.711	88.7	52	29	**132.4**	13	11	9	corrected
*61	C	SO-11B		573.3		0.1	1.016	1.019	28163.8	35	36	**>method**				uncorrected
*61	D	SO-16B		456.6		1.4	1.072	0.553	571.9	41	26	**86.6**	5	5	6	uncorrected
*62	A	11-26-A		672.8		1.6	1.125	0.769	1095.7	9	20	**152.2**	19	15		uncorrected
*62	B	11-26-E		746.8		23.3	1.109	0.737	77.4	6	14	**140.1**	19	16		corrected
*62	C	SO-11-A		318.4		4.7	1.022	1.000	880.7	51	53	**>method**				uncorrected
*62	D	9-25-EF		671.4		4.7	1.062	0.404	180.0	19	26	**55.9**	3	3		uncorrected
63*	A	11-28-A		1569.8		0.7	1.069	0.325	2434.0	28	18	**42.5**	2	2	4	uncorrected

Lab	Series	sample	Uicp ppb	U-a ppb	Thicp ppb	Th-a ppb	234U/238U	230T/234U	230T/232T	Yld-U	Yld-Th%	AGE ky	error+ ky	error- ky	% error	correction
63*	B	11-28-D		1930.2		12.6	1.050	0.370	175.7	34	24	**50.1**	2	2	3	uncorrected
*65	A	HT-12A		224.4		1.2	1.122	0.048	30.8	7	49	**5.3**	1	1	11	corrected
*65	B	HT-11A		422.3		6.5	1.088	0.022	6.3	38	49	**2.4**	0	0	13	corrected
*65	C	SO-24Y		1004.4		1.5	1.043	0.847	80.2	8	25	**198.4**	31	23	14	corrected
*65	D	SO-28Y		566.4		1.5	1.153	0.503	664.9	34	63	**74.6**	3	3	4	uncorrected
*66	A	SO-21B	550.0	487.3	13.0	7.6	1.021	1.021	196.3	35	66	**>method**				uncorrected
*66	B	CC-1A		157.7		47.3	2.243	0.391	10.0	34	45	**68.0**	4	3	5	
*66	C	HT-1A	415.0	401.5	**70.0**	**1.2**	1.004	1.030	422.9	37	10	**>method**				uncorrected
*66	D	HT-1B	160.0	162.3	**30.0**	**1.2**	1.049	0.890	381.1	41	16	**230.0**	59	36	21	uncorrected
*67	A	HT-13A	410.0	364.5	15.0	1.2	1.106	0.023	24.7	17	60	**2.5**	0	0	11	corrected
*67	B	HT-20A		569.2		4.0	1.174	0.640	318.0	41	60	**107.3**	5	4	4	uncorrected
*67	C	HT-23A	310.0	302.4	<10	~0	1.158	0.678	5812.0	41	55	**118.6**	6	6	5	uncorrected
*67	D	HT-21A	460.0	476.9	<10	~0	1.122	0.584	2563.0	46	16	**93.3**	5	5	5	uncorrected
*69	B	HT-9A	345.0	334.3	**15.0**	**0.9**	1.084	0.068	85.0	46	46	**7.6**	1	1	7	corrected
*69	C	SO-22A	450.0	358.0	50.0	29.5	1.003	0.990	35.5	52	11	**>287**				corrected
*69	D	SO-22B	340.0	329.1	<10	1.3	0.984	0.983	711.6	25	54	**>304**				uncorrected
*69	E	SO-22C	480.0	399.0	<10	1.2	0.986	0.995	983.1	34	51	**>method**				uncorrected
*71	A	HT-14B	269.0	207.2	2.1	0.6	1.080	0.087	92.9	33	56	**9.8**	1	1	6	corrected
*71	B	HT-14A	237.0	217.4	2.5	3.4	1.126	0.096	21.9	21	53	**11.0**	1	1	6	corrected
*71	C	HT-18E	666.0	560.3	4.3	0.0	1.121	0.846	366.8	31	9	**190.1**	20	16	9	uncorrected
*71	D	HT-18F	551.0	471.8	1.8	0.0	1.149	0.754	57157.0	28	50	**144.9**	7	7	5	uncorrected
*72	A	SO-17A	371.0	320.3	4.6	0.2	1.051	0.309	1311.0	53	43	**40.1**	2	2	6	uncorrected
*72	B	SO-21A	364.0	337.2	2.7	-0.2	0.976	0.880	647.0	35	11	**236.2**	88	44	28	uncorrected
*72	C	SO-29Y	448.0	374.5	6.1	0.2	1.076	0.729	4704.3	53	34	**138.6**	12	11	8	uncorrected
*72	D	SO-19B	478.0	405.0	11.0	4.4	1.006	0.987	271.3	47	51	**>317**				uncorrected
*73	A	HT-24A	580.0	511.4	1.7	1.4	0.996	0.996	9519.0	28	52	**676.6**		325		uncorrected
*73	B	HT-15A	335.0	298.9	9.6	5.4	1.071	0.008	3.2	32	29	**0.9**	0	0	53	*corrected
*73	C	SO-15A	282.0	255.3	8.2	1.7	1.087	0.695	851.0	27	22	**126.0**	15	13	11	uncorrected
*73	D	HT-18A	531.0	460.6	3.2	~0	1.003	1.009	5108.0	22	43	**>method**				uncorrected
*74	A	HT-24D	674.0	585.0	1.5	1.9	1.009	1.039	970.1	42	15	**>method**				uncorrected
*74	B	HT 18C	411.0	315.0	5.7	~0	1.131	0.922	3408.0	38	57	**243.2**	61	37	20	uncorrected
*74	C	HT 24B		250.3		~0	1.053	1.048	1019.0	48	34	**>method**				uncorrected
*74	D	HT 24C		366.7		0.0	1.068	0.960	40007.0	40	40	**>242**				uncorrected
*77	A	SO-39Y	627.0	637.4	2.1	0.6	1.062	0.452	1515.3	10	10	**64.9**	7	6	10	uncorrected
*77	B	SO-38B	426.0	410.4	5.9	2.8	1.053	0.488	220.0	34	63	**72.3**	4	4	5	uncorrected
*77	C	SO-40A	516.0	439.7	5.6	~0	1.170	0.591	862.1	43	46	**94.4**	5	5	5	uncorrected

Lab	Series	sample	Uicp ppb	U-a ppb	Thicp ppb	Th-a ppb	234U/238U	230T/234U	230T/232T	Yld-U	Yld-Th%	AGE ky	error+ ky	error- ky	% error	correction
*77	D	SO-40B	432.0	403.3	5.1	~0	1.200	0.430	2153.0	45	61	60.1	3	3	4	uncorrected
*78	A	SO-29Y	448.0	437.1	6.1	10.1	1.101	0.691	97.6	30	22	124.4	17	14	13	corrected
*78	B	SO-31B	297.0	248.9	11.2	5.7	1.119	0.642	92.9	40	42	108.9	12	11	11	corrected
*78	C	SO-35B	590.0	530.5	3.0	~0	1.110	0.963	7280.5	32	19	>method				uncorrected
*78	D	SO-34A	273.0	211.8	5.4	~0	1.114	1.019	1174.0	24	51	>method				uncorrected
*79	A	SO-33A	215.0	529.2	15.0	18.0	1.052	0.943	86.0	12	10	>217				corrected
*79	B	SO-36A	350.0	356.2	30.0	14.9	0.994	1.076	75.4	26	55	>method				corrected
*79	C	SO-38C	####	946.0	2.8	4.3	1.026	0.001	4.1	19	12	0.1	0	0	440	corrected
*79	D	SO-36B	230.0	219.3	15.0	4.3	1.039	0.970	151.6	19	62	>method				uncorrected
*85	A	SO-37Y	320.0	326.5	10.0	3.6	1.090	0.908	266.8	37	54	237.8	43	30	15	uncorrected
*85	B	SO-43A	590.0	662.9	10.0	3.2	1.043	0.994	630.7	40	22	>method				uncorrected
*85	C	SO-43B	730.0	642.6	15.0	0.1	1.158	0.726	2382.2	32	23	134.5	12	11	8	uncorrected
*85	D	SO-42Y	340.0	373.0	10.0	0.1	1.033	1.001	10478.4	41	30	>method				uncorrected
*86	A	SO-44A	380.0	436.5	<10	2.4	1.095	0.484	282.9	40	30	71.2	5	5	7	uncorrected
*86	B	HT-10A	337.0	376.4	30.0	5.3	1.060	0.025	7.4	29	30	2.8	1	1	20	corrected
*86	C	HT-19A	495.0	503.0	20.0	0.1	1.266	0.399	1563.0	29	24	54.3	3	3	6	uncorrected
*86	D	SO-32B	590.0	750.7	40.0	0.1	1.076	0.001	25.9	42	22	0.1	0	0	149	corrected
*87	A	HT-18H	530.0	545.3	25.0	3.5	1.146	0.594	315.0	48	18	95.6	7	6	7	uncorrected
*87	B	HT-7A	613.0	333.3	58.0	2.8	1.165	0.732	295.7	36	46	136.2	11	10	8	uncorrected
*87	C	S0-4B	?	267.5		0.8	1.189	0.884	985.1	38	35	>method				uncorrected
*87	D	SO-19A	665.0	594.0	71.0	91.8	1.065	0.999	20.2	24	51	>method				corrected

Table 2. Collapses in chronological order

Collapses	lamina dated	Age[ky]	plus [ky]	minus [ky]	TIMS [ky]	Min or max	Age-profile[ky]	Possible correlation	
SO-32	B	0.12	0.18	0.18		min			Histor-
SO-38	C	0.072	0.32	0.316	0.063+-0.003	min	0.9		ical
HT-13	A	2.5	0.3	0.3		min	2.6	Dead	
HT-11	A	2.4	0.3	0.3		min	3.8	Sea	
HT-10	A	2.8	0.57	0.56		min	4.7		
HT-15	A	0.87	0.46	0.46	1.82+-0.044	min	5.1		
HT-12	A	5.3	0.6	0.6	3.648+-0.113	min	5.3		
HT-14	A	11	0.6	0.6		min	13		
HT-9	A	7.6	0.6	0.5		min	13.5		
.1-6	B					min	35		
SO-7	D	41	4	3		min	44		
	C	50	4	3		max	44.1		
SO-17	A	40	2.5	2.4		min	48	Lisan	
HT-19	A	54	3	3		min	53.5		
SO-39	Y	65	6	6		max	64		
SO-44	A	71	5	5		min			
SO-14	A	74	3	3		min	71		
SO-28	Y	75	3	3		max	72		
HT-18	I					min	95		
	H	96	6 ?			max	95		
SO-40	B	60	3	3		min	100		
	A	94	5	5		max	104		
HT-21	A	93	5	5		min	107		
SO-31	B	109	12	11		min	107		
SO-15	AA	126	15	13		min	128		
SO-8	B	120	11	9		min	128		Samra
HT-23	A	119	6	6		min	135		
HT-20	A	107	5	4		min	144		
SO-43	B	135	12	11		min	144		
HT-7	A	136	11	10		min	144		
HT-18	E	190	20	16		max	144		
	F	145	7	6		min			
SO-13	B	132	13	12		min	160		
SO-24	Y	198	31	23		max			
HT-1	B	230	59	36		min			
HT-18	B					min			
HT-18	C	243	61	37		min			
SO-33	A	>217				min			
HT-24	C	>242	65			min			
SO-9	A	>313							
SO-36	B	>LIM							
SO-11	A	>LIM							
SO-22	C	>LIM	160			min			
SO-34	A	>LIM				min			
SO-35	B	>LIM				min			

PUBLICATION DOCUMENTATION PAGE

1. Publication No. ES - 26-01	2.	3. Recipient Accession No.
4. Title and Subtitle Earthquakes dated by damaged speleothems		5. Publication Date 11/11/01 6. Performing Organiz. Code
7. Author(s) E. Kagan, A. Agnon, M. Bar-Matthews, A. Ayalon		8. Performing Organiz. Rep. No. GSI/33/01
9. Performing Organization Name and Address Institute of Earth Sciences, Hebrew University of Jerusalem		10. Project / Task / Work Unit No. 11. Contract No. 20-17-028
12. Sponsoring Organisation(s) Name and Address (a) Ministry of Energy and Infrastructure Earth Science Administration P. O. Box 13106, 91130 Jerusalem (b)		13. Type of Report and Period Covered Annual Report. 11/00-10/01 14. Sponsoring Organiz. Code
15. Supplementary Notes		

16. Abstract (Limit 200 Words)

The Soreq and Har-Tuv Caves, located 60 km west of the Dead Sea Fault, record earthquake damage from transform ruptures and smaller local intraplate events. These caves contain damaged cave deposits of all types, sizes, and ages. Subsequent precipitation on damaged speleothems constrains ages of collapse. Comprehensive maps of the Soreq Har-Tuv Caves demonstrate (1) orientation and length of fractures, (2) orientation of collapsed and deformed speleothems and ceiling blocks; EW collapse orientation is dominant. Fallen large stalagmites, collapsed ceilings, and the speleothems that have grown on them were sampled. Unconformities were identified between the collapses and the in-situ regrowth. Laminae above and below the unconformity were separated and dated by alpha counting at the Geological Survey of Israel. Ninety samples of speleothem calcite were dated using alpha 230Th/234U (<350 ky). Correlation with the well-dated 185 ky stable isotope profile of the Soreq Cave vastly improves alpha-method ages. Nineteen events were dated. Of the 5 collapses in the Holocene all seem correlated to historically or geologically documented earthquakes. Of the 6 collapses between 20-80 ky, 5 correlate with mixed layers in the Lisan Fm. Older events represent the only paleoseismic record of its age studied in the region.

17. Identifiers / Keywords / Descriptors
Earthquakes, Speleothems, Cave Deposits, Paleoseismicity, U-Th dating, Wiggle-matching-stable isotope correlation

18. Avialbility Statement	19. Security Class (This Report)	21. No. of Pages
	20. Security Class (This Page)	22. Price